

Visual Appearance of Nanocrystal-Based Luminescent Solar Concentrators

Volume 12 · Issue 6 | March (II) 2019

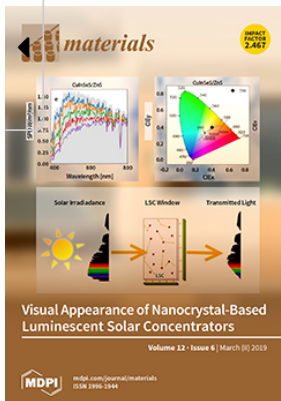
Affiliated Society:



(https://serve.mdpi.com/www/my_files/cliik.php?oaparams=0bar)

Materials, Volume 12, Issue 6 (March-2 2019)

– 161 articles



Cover Story ([view full-size image](#)

(/files/uploaded/covers/materials/big_cover-materials-v12-i6.png):

The Luminescent Solar Concentrator (LSC) is a technological device that can revolutionize the way we harvest solar energy in the urban environment as windows and facades can be turned in to solar energy generators. The active element of the LSC, in this case a CuInSeS/ZnS nanocrystal, absorbs part of the solar spectrum in order to be utilized for energy production and the rest is used for the internal illumination of the building itself. Depending on the concentration of CuInSeS/ZnS, the solar spectrum and especially the visible part will be affected in a different way causing a mild color distortion compared to the natural daylight. [View this paper \(https://www.mdpi.com/1996-1944/12/6/885\)](#).

(<https://www.mdpi.com/1996-1944/12/6/885>)

- Issues are regarded as officially published after their release is announced to the [table of contents alert mailing list \(/journal/materials/toc-alert\)](#).
- You may [sign up for e-mail alerts \(/journal/materials/toc-alert\)](#) to receive table of contents of newly released issues.
- PDF is the official format for papers published in both, html and pdf forms. To view the papers in pdf format, click on the "PDF Full-text" link, and use the free [Adobe Reader \(https://www.adobe.com/\)](https://www.adobe.com/) to open them.

Order results

Publication Date

Result details

Compact

[Show export options](#) 

Open Access Article

  (</1996-1944/12/6/999/pdf>)

[Investigations of Machining Characteristics in the Upgraded MQL-Assisted Turning of Pure Titanium Alloys Using Evolutionary Algorithms \(/1996-1944/12/6/999\)](#)

Materials **2019**, *12*(6), 999; <https://doi.org/10.3390/ma12060999>

(<https://doi.org/10.3390/ma12060999>) - 26 Mar 2019

Cited by 29 (/1996-1944/12/6/999#citedby) | Viewed by 1729



Open Access Article



(/1996-1944/12/6/998/pdf)

Lifing the Effects of Crystallographic Orientation on the Thermo-Mechanical Fatigue Behaviour of a Single-Crystal Superalloy (/1996-1944/12/6/998)

Materials **2019**, *12*(6), 998; <https://doi.org/10.3390/ma12060998>

(<https://doi.org/10.3390/ma12060998>) - 26 Mar 2019

Viewed by 1328

Open Access Article



(/1996-1944/12/6/997/pdf)

Seismic Behavior of Superelastic Shape Memory Alloy Spring in Base Isolation System of Multi-Story Steel Frame (/1996-1944/12/6/997)

Materials **2019**, *12*(6), 997; <https://doi.org/10.3390/ma12060997>

(<https://doi.org/10.3390/ma12060997>) - 26 Mar 2019

Cited by 9 (/1996-1944/12/6/997#citedby) | Viewed by 1682

Open Access Article



(/1996-1944/12/6/996/pdf)

Ternary Blended Binder for Production of a Novel Type of Lightweight Repair Mortar (/1996-1944/12/6/996)

Materials **2019**, *12*(6), 996; <https://doi.org/10.3390/ma12060996>

(<https://doi.org/10.3390/ma12060996>) - 26 Mar 2019

Cited by 14 (/1996-1944/12/6/996#citedby) | Viewed by 1418

Open Access Article



(/1996-1944/12/6/995/pdf)

Evaluating the Quality Surface Performance of Additive Manufacturing Systems: Methodology and a Material Jetting Case Study (/1996-1944/12/6/995)

Materials **2019**, *12*(6), 995; <https://doi.org/10.3390/ma12060995>

(<https://doi.org/10.3390/ma12060995>) - 26 Mar 2019

Cited by 21 (/1996-1944/12/6/995#citedby) | Viewed by 2084

Open Access Article



(/1996-1944/12/6/994/pdf)

3D-Printed Polyester-Based Prototypes for Cosmetic Applications—Future Directions at the Forensic Engineering of Advanced Polymeric Materials (/1996-1944/12/6/994)

Materials **2019**, *12*(6), 994; <https://doi.org/10.3390/ma12060994>

(<https://doi.org/10.3390/ma12060994>) - 26 Mar 2019

Cited by 4 (/1996-1944/12/6/994#citedby) | Viewed by 1269

Open Access Article



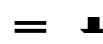
(/1996-1944/12/6/993/pdf)

Microstructure and Thermal Insulation Property of Silica Composite Aerogel (/1996-1944/12/6/993)



Materials **2019**, *12*(6), 993; <https://doi.org/10.3390/ma12060993>




(<https://doi.org/10.3390/ma12060993>) - 26 Mar 2019

Cited by 9 (/1996-1944/12/6/993#citedby) | Viewed by 1877



Open Access Article

  [\(/1996-1944/12/6/992/pdf\)](#)



Experimental Study on Mechanical Characteristics and Fracture Patterns of Unfrozen/Freezing Saturated Coal and Sandstone [\(/1996-1944/12/6/992\)](#)   

Materials **2019**, *12*(6), 992; <https://doi.org/10.3390/ma12060992>

<https://doi.org/10.3390/ma12060992> - 26 Mar 2019

Cited by 4 [\(/1996-1944/12/6/992#citedby\)](#) | Viewed by 1112

Open Access Feature Paper Article

  [\(/1996-1944/12/6/991/pdf\)](#)


Laser Polishing of Additive Manufactured 316L Stainless Steel Synthesized by Selective Laser Melting [\(/1996-1944/12/6/991\)](#)

Materials **2019**, *12*(6), 991; <https://doi.org/10.3390/ma12060991>

<https://doi.org/10.3390/ma12060991> - 26 Mar 2019

Cited by 18 [\(/1996-1944/12/6/991#citedby\)](#) | Viewed by 1931

Open Access Article

  [\(/1996-1944/12/6/990/pdf\)](#)

Thermal, Mechanical, Viscoelastic and Morphological Properties of Poly(lactic acid) based Biocomposites with Potato Pulp Powder Treated with Waxes [\(/1996-1944/12/6/990\)](#)

Materials **2019**, *12*(6), 990; <https://doi.org/10.3390/ma12060990>

<https://doi.org/10.3390/ma12060990> - 26 Mar 2019

Cited by 16 [\(/1996-1944/12/6/990#citedby\)](#) | Viewed by 1383

Open Access Article

  [\(/1996-1944/12/6/989/pdf\)](#)

Self-Flushing in EDM Drilling of Ti6Al4V Using Rotating Shaped Electrodes [\(/1996-1944/12/6/989\)](#)

Materials **2019**, *12*(6), 989; <https://doi.org/10.3390/ma12060989>

<https://doi.org/10.3390/ma12060989> - 26 Mar 2019

Cited by 9 [\(/1996-1944/12/6/989#citedby\)](#) | Viewed by 1951

Open Access Article

  [\(/1996-1944/12/6/988/pdf\)](#)

Aging Mechanism of a Diatomite-Modified Asphalt Binder Using Fourier-Transform Infrared (FTIR) Spectroscopy Analysis [\(/1996-1944/12/6/988\)](#)

Materials **2019**, *12*(6), 988; <https://doi.org/10.3390/ma12060988>

<https://doi.org/10.3390/ma12060988> - 26 Mar 2019

Cited by 6 [\(/1996-1944/12/6/988#citedby\)](#) | Viewed by 1322

Open Access Article

  [\(/1996-1944/12/6/1001/pdf\)](#)

An Investigation on Microstructure, Texture and Mechanical Properties of AZ80 Mg Alloy Processed by Annular Channel Angular Extrusion [\(/1996-1944/12/6/1001\)](#)

Materials **2019**, *12*(6), 1001; <https://doi.org/10.3390/ma12061001>

<https://doi.org/10.3390/ma12061001> - 26 Mar 2019

Cited by 8 [\(/1996-1944/12/6/1001#citedby\)](#) | Viewed by 1240

Open Access Article

  [\(/1996-1944/12/6/1000/pdf\)](#)

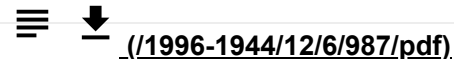
Preparation, Characterization, and Stability Evaluation of Taste-Masking Lacosamide Microparticles (/1996-1944/12/6/1000)

Materials 2019, 12(6), 1000; <https://doi.org/10.3390/ma12061000>

(<https://doi.org/10.3390/ma12061000>) - 26 Mar 2019

Cited by 3 (</1996-1944/12/6/1000#citedby>) | Viewed by 1344

Open Access Article



(</1996-1944/12/6/987/pdf>)

Corrosion Resistance of Stainless Steels Intended to Come into Direct or Prolonged Contact with the Skin (/1996-1944/12/6/987)

Materials 2019, 12(6), 987; <https://doi.org/10.3390/ma12060987>

(<https://doi.org/10.3390/ma12060987>) - 25 Mar 2019

Cited by 3 (</1996-1944/12/6/987#citedby>) | Viewed by 1137

Open Access Article



(</1996-1944/12/6/986/pdf>)

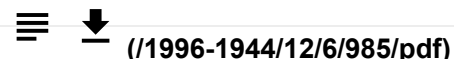
Control of Dopant Distribution in Yttrium-Doped Bioactive Glass for Selective Internal Radiotherapy Applications Using Spray Pyrolysis (/1996-1944/12/6/986)

Materials 2019, 12(6), 986; <https://doi.org/10.3390/ma12060986>

(<https://doi.org/10.3390/ma12060986>) - 25 Mar 2019

Cited by 3 (</1996-1944/12/6/986#citedby>) | Viewed by 1190

Open Access Article



(</1996-1944/12/6/985/pdf>)

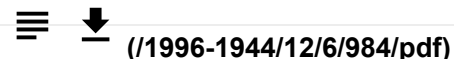
Influence of PMMA on All-Inorganic Halide Perovskite CsPbBr₃ Quantum Dots Combined with Polymer Matrix (/1996-1944/12/6/985)

Materials 2019, 12(6), 985; <https://doi.org/10.3390/ma12060985>

(<https://doi.org/10.3390/ma12060985>) - 25 Mar 2019

Cited by 13 (</1996-1944/12/6/985#citedby>) | Viewed by 2277

Open Access Article



(</1996-1944/12/6/984/pdf>)

Preparation and Physical Properties of High-Belite Sulphoaluminate Cement-Based Foam Concrete Using an Orthogonal Test (/1996-1944/12/6/984)

Materials 2019, 12(6), 984; <https://doi.org/10.3390/ma12060984>

(<https://doi.org/10.3390/ma12060984>) - 25 Mar 2019

Cited by 3 (</1996-1944/12/6/984#citedby>) | Viewed by 1356

Open Access Article



(</1996-1944/12/6/983/pdf>)

Artificial Intelligence Approaches for Prediction of Compressive Strength of Geopolymer Concrete (/1996-1944/12/6/983)

Materials 2019, 12(6), 983; <https://doi.org/10.3390/ma12060983>

(<https://doi.org/10.3390/ma12060983>) - 25 Mar 2019

Cited by 61 (</1996-1944/12/6/983#citedby>) | Viewed by 3145

Open Access Letter



(</1996-1944/12/6/982/pdf>)

A Statistical Model of Cleavage Fracture Toughness of Ferritic Steel DIN 22NiMoCr37 at Different Temperatures (/1996-1944/12/6/982)

Materials 2019, 12(6), 982; <https://doi.org/10.3390/ma12060982>

(<https://doi.org/10.3390/ma12060982>) - 25 Mar 2019

Cited by 6 ([/1996-1944/12/6/982#citedby](#)) | Viewed by 1128



Open Access Article

[\(/1996-1944/12/6/981/pdf\)](#)

Influence of W Addition on Microstructure and Mechanical Properties of Al-12%Si Alloys (/1996-1944/12/6/981)

Materials 2019, 12(6), 981; <https://doi.org/10.3390/ma12060981>

(<https://doi.org/10.3390/ma12060981>) - 25 Mar 2019

Cited by 16 ([/1996-1944/12/6/981#citedby](#)) | Viewed by 1313

Open Access Article

[\(/1996-1944/12/6/980/pdf\)](#)

Influence of the Elastic Modulus on the Osseointegration of Dental Implants (/1996-1944/12/6/980)

Materials 2019, 12(6), 980; <https://doi.org/10.3390/ma12060980>

(<https://doi.org/10.3390/ma12060980>) - 25 Mar 2019

Cited by 13 ([/1996-1944/12/6/980#citedby](#)) | Viewed by 1747

Open Access Article

[\(/1996-1944/12/6/979/pdf\)](#)

The Effect of Hemostatic Agents on the Retention Strength of Zirconia Crowns Luted to Dentin Abutments (/1996-1944/12/6/979)

Materials 2019, 12(6), 979; <https://doi.org/10.3390/ma12060979>

(<https://doi.org/10.3390/ma12060979>) - 25 Mar 2019

Viewed by 1156

Open Access Review

[\(/1996-1944/12/6/978/pdf\)](#)

Graphene-Based Inks for Printing of Planar Micro-Supercapacitors: A Review (/1996-1944/12/6/978)

Materials 2019, 12(6), 978; <https://doi.org/10.3390/ma12060978>

(<https://doi.org/10.3390/ma12060978>) - 25 Mar 2019

Cited by 14 ([/1996-1944/12/6/978#citedby](#)) | Viewed by 1713

Open Access Article

[\(/1996-1944/12/6/977/pdf\)](#)

Bending Properties of Mg Alloy Tailored Arc-Heat-Treated Blanks (/1996-1944/12/6/977)

Materials 2019, 12(6), 977; <https://doi.org/10.3390/ma12060977>

(<https://doi.org/10.3390/ma12060977>) - 25 Mar 2019

Viewed by 1018

Open Access Article

[\(/1996-1944/12/6/976/pdf\)](#)

Regulating the Expansion Characteristics of Cementitious Materials Using Blended MgO-Type Expansive Agent (/1996-1944/12/6/976)



Materials 2019, 12(6), 976; <https://doi.org/10.3390/ma12060976>

(<https://doi.org/10.3390/ma12060976>) - 25 Mar 2019

Cited by 3 ([/1996-1944/12/6/976#citedby](#)) | Viewed by 1045



Open Access Article

  [\(/1996-1944/12/6/975/pdf\)](#)



Variation of the Pore Morphology during the Early Age in Plain and Fiber-Reinforced High-Performance Concrete under Moisture-Saturated Curing [\(/1996-1944/12/6/975\)](#)  

Materials **2019**, *12*(6), 975; <https://doi.org/10.3390/ma12060975>

[\(/https://doi.org/10.3390/ma12060975\)](https://doi.org/10.3390/ma12060975) - 24 Mar 2019

Cited by 2 [\(/1996-1944/12/6/975#citedby\)](#) | Viewed by 1053

Open Access Article

  [\(/1996-1944/12/6/974/pdf\)](#)

An Approach to the Uniform Dispersion of Graphene Nanosheets in Powder Metallurgy Nickel-Based Superalloy [\(/1996-1944/12/6/974\)](#)

Materials **2019**, *12*(6), 974; <https://doi.org/10.3390/ma12060974>

[\(/https://doi.org/10.3390/ma12060974\)](https://doi.org/10.3390/ma12060974) - 24 Mar 2019

Cited by 1 [\(/1996-1944/12/6/974#citedby\)](#) | Viewed by 1464

Open Access Article

  [\(/1996-1944/12/6/973/pdf\)](#)

Effects of High Temperature on the Burst Process of Carbon Fiber/PVA Fiber High-Strength Concretes [\(/1996-1944/12/6/973\)](#)

Materials **2019**, *12*(6), 973; <https://doi.org/10.3390/ma12060973>

[\(/https://doi.org/10.3390/ma12060973\)](https://doi.org/10.3390/ma12060973) - 24 Mar 2019

Cited by 4 [\(/1996-1944/12/6/973#citedby\)](#) | Viewed by 1305

Open Access Article

  [\(/1996-1944/12/6/972/pdf\)](#)


CH₄ Adsorption Probability on GaN(0001) and (000-1) during Metalorganic Vapor Phase Epitaxy and Its Relationship to Carbon Contamination in the Films [\(/1996-1944/12/6/972\)](#)

Materials **2019**, *12*(6), 972; <https://doi.org/10.3390/ma12060972>

[\(/https://doi.org/10.3390/ma12060972\)](https://doi.org/10.3390/ma12060972) - 23 Mar 2019

Cited by 5 [\(/1996-1944/12/6/972#citedby\)](#) | Viewed by 1355

Open Access Article

  [\(/1996-1944/12/6/971/pdf\)](#) 

Flexible Carbon Nanotube-Based Polymer Electrode for Long-Term Electrocardiographic Recording [\(/1996-1944/12/6/971\)](#)

Materials **2019**, *12*(6), 971; <https://doi.org/10.3390/ma12060971>

[\(/https://doi.org/10.3390/ma12060971\)](https://doi.org/10.3390/ma12060971) - 23 Mar 2019

Cited by 12 [\(/1996-1944/12/6/971#citedby\)](#) | Viewed by 1340

Open Access Article

  [\(/1996-1944/12/6/970/pdf\)](#) 

Influence of Porous Dressings Based on Butyric-Acetic Chitin Co-Polymer on Biological Processes In Vitro and In Vivo [\(/1996-1944/12/6/970\)](#)

Materials **2019**, *12*(6), 970; <https://doi.org/10.3390/ma12060970>

[\(/https://doi.org/10.3390/ma12060970\)](https://doi.org/10.3390/ma12060970) - 23 Mar 2019

Cited by 5 [\(/1996-1944/12/6/970#citedby\)](#) | Viewed by 972

Open Access Communication

  [\(/1996-1944/12/6/969/pdf\)](#)

Na⁺K⁺ Hybrid Battery Based on a Sulfurized Polyacrylonitrile Cathode (/1996-1944/12/6/969)

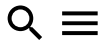
Materials **2019**, 12(6), 969; <https://doi.org/10.3390/ma12060969>

(<https://doi.org/10.3390/ma12060969>) - 23 Mar 2019

Cited by 1 (/1996-1944/12/6/969#citedby) | Viewed by 1030



(/toggle_desktop_layout_cookie)



Open Access Article



(/1996-1944/12/6/968/pdf)

Degradation of Phenol Using Peroxymonosulfate Activated by a High Efficiency and Stable CoMgAl-LDH Catalyst (/1996-1944/12/6/968)

Materials **2019**, 12(6), 968; <https://doi.org/10.3390/ma12060968>

(<https://doi.org/10.3390/ma12060968>) - 23 Mar 2019

Cited by 3 (/1996-1944/12/6/968#citedby) | Viewed by 1101

Open Access Article



(/1996-1944/12/6/967/pdf)

First-Principles Study on the Mechanical Properties and Electronic Structure of V Doped WCoB and W₂CoB₂ Ternary Borides (/1996-1944/12/6/967)

Materials **2019**, 12(6), 967; <https://doi.org/10.3390/ma12060967>

(<https://doi.org/10.3390/ma12060967>) - 22 Mar 2019

Cited by 9 (/1996-1944/12/6/967#citedby) | Viewed by 1179

Open Access Article



(/1996-1944/12/6/966/pdf)

Effects of the Thickness of N,N'-diphenyl-N,N'-di(m-tolyl)-benzidine on the Electro-Optical Characteristics of Organic Light-Emitting Diodes (/1996-1944/12/6/966)

Materials **2019**, 12(6), 966; <https://doi.org/10.3390/ma12060966>

(<https://doi.org/10.3390/ma12060966>) - 22 Mar 2019

Viewed by 918

Open Access Article



(/1996-1944/12/6/965/pdf)

Influence of the Loading Speed on the Ductility Properties of Corroded Reinforcing Bars in Concrete (/1996-1944/12/6/965)

Materials **2019**, 12(6), 965; <https://doi.org/10.3390/ma12060965>

(<https://doi.org/10.3390/ma12060965>) - 22 Mar 2019

Cited by 2 (/1996-1944/12/6/965#citedby) | Viewed by 881

Open Access Article



(/1996-1944/12/6/964/pdf)



A Semi-Empirical Deflection-Based Method for Crack Width Prediction in Accelerated Construction of Steel Fibrous High-Performance Composite Small Box Girder (/1996-1944/12/6/964)

Materials **2019**, 12(6), 964; <https://doi.org/10.3390/ma12060964>

(<https://doi.org/10.3390/ma12060964>) - 22 Mar 2019

Cited by 1 (/1996-1944/12/6/964#citedby) | Viewed by 1497

Open Access Article



(/1996-1944/12/6/963/pdf)

Inspection of Reactor Steel Degradation by Magnetic Adaptive Testing (/1996-1944/12/6/963)

Materials 2019, 12(6), 963; <https://doi.org/10.3390/ma12060963>

(<https://doi.org/10.3390/ma12060963>) - 22 Mar 2019

Cited by 1 (</1996-1944/12/6/963#citedby>) | Viewed by 889



Open Access Feature Paper Article

(</1996-1944/12/6/962/pdf>)

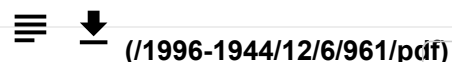
UV Irradiated Graphene-Based Nanocomposites: Change in the Mechanical Properties by Local HarmoniX Atomic Force Microscopy Detection (</1996-1944/12/6/962>)

Materials 2019, 12(6), 962; <https://doi.org/10.3390/ma12060962>

(<https://doi.org/10.3390/ma12060962>) - 22 Mar 2019

Cited by 5 (</1996-1944/12/6/962#citedby>) | Viewed by 1118

Open Access Article



(</1996-1944/12/6/961/pdf>)

Effect of Temperature, Pressure, and Chemical Composition on the Electrical Conductivity of Schist: Implications for Electrical Structures under the Tibetan Plateau (</1996-1944/12/6/961>)

Materials 2019, 12(6), 961; <https://doi.org/10.3390/ma12060961>

(<https://doi.org/10.3390/ma12060961>) - 22 Mar 2019

Cited by 1 (</1996-1944/12/6/961#citedby>) | Viewed by 998

Open Access Article



(</1996-1944/12/6/960/pdf>)

The Effect of Epoxy Polymer Addition in Sn-Ag-Cu and Sn-Bi Solder Joints (</1996-1944/12/6/960>)

Materials 2019, 12(6), 960; <https://doi.org/10.3390/ma12060960>

(<https://doi.org/10.3390/ma12060960>) - 22 Mar 2019

Cited by 2 (</1996-1944/12/6/960#citedby>) | Viewed by 1157

Open Access Article



(</1996-1944/12/6/959/pdf>)

Study on Dynamic Response Characteristics of Saturated Asphalt Pavement under Multi-Field Coupling (</1996-1944/12/6/959>)

Materials 2019, 12(6), 959; <https://doi.org/10.3390/ma12060959>

(<https://doi.org/10.3390/ma12060959>) - 22 Mar 2019

Cited by 1 (</1996-1944/12/6/959#citedby>) | Viewed by 855

Open Access Article



(</1996-1944/12/6/958/pdf>)

Fabrication of Nanopillar Crystalline ITO Thin Films with High Transmittance and IR Reflectance by RF Magnetron Sputtering (</1996-1944/12/6/958>)

Materials 2019, 12(6), 958; <https://doi.org/10.3390/ma12060958>

(<https://doi.org/10.3390/ma12060958>) - 22 Mar 2019

Cited by 4 (</1996-1944/12/6/958#citedby>) | Viewed by 1351

Open Access Feature Paper Article



(</1996-1944/12/6/957/pdf>)

Damage from Coexistence of Ferroelectric and Antiferroelectric Domains and Clustering of O Vacancies in PZT: An Elastic and Raman Study (</1996-1944/12/6/957>)

Materials 2019, 12(6), 957; <https://doi.org/10.3390/ma12060957>

(<https://doi.org/10.3390/ma12060957>) - 22 Mar 2019

Cited by 2 (/1996-1944/12/6/957#citedby) | Viewed by 975



Open Access Article



./1996-1944/12/6/956/pdf)

Non-Destructive Evaluation of Impacted CFRP by IR Thermography (/1996-1944/12/6/956)

Materials **2019**, *12*(6), 956; <https://doi.org/10.3390/ma12060956>

(<https://doi.org/10.3390/ma12060956>) - 22 Mar 2019

Cited by 4 (/1996-1944/12/6/956#citedby) | Viewed by 721

Open Access Article



./1996-1944/12/6/955/pdf)

Numerical Analysis and Its Laboratory Verification in Bending Test of Glue Laminated Timber Pre-Cracked Beam (/1996-1944/12/6/955)

Materials **2019**, *12*(6), 955; <https://doi.org/10.3390/ma12060955>

(<https://doi.org/10.3390/ma12060955>) - 22 Mar 2019

Cited by 1 (/1996-1944/12/6/955#citedby) | Viewed by 1100

Open Access Article



./1996-1944/12/6/954/pdf)

Improved Performance of Graphene in Heat Dissipation when Combined with an Orientated Magnetic Carbon Fiber Skeleton under Low-Temperature Thermal Annealing (/1996-1944/12/6/954)

Materials **2019**, *12*(6), 954; <https://doi.org/10.3390/ma12060954>

(<https://doi.org/10.3390/ma12060954>) - 22 Mar 2019

Cited by 1 (/1996-1944/12/6/954#citedby) | Viewed by 1085

Open Access Article



./1996-1944/12/6/953/pdf)

The Effect of Phase Angle on the Thermo-Mechanical Fatigue Life of a Titanium Metal Matrix Composite (/1996-1944/12/6/953)

Materials **2019**, *12*(6), 953; <https://doi.org/10.3390/ma12060953>

(<https://doi.org/10.3390/ma12060953>) - 22 Mar 2019

Viewed by 1294

Open Access Review



./1996-1944/12/6/952/pdf)

Graphene Nanomaterials-Based Radio-Frequency/Microwave Biosensors for Biomaterials Detection (/1996-1944/12/6/952)

Materials **2019**, *12*(6), 952; <https://doi.org/10.3390/ma12060952>

(<https://doi.org/10.3390/ma12060952>) - 21 Mar 2019

Cited by 6 (/1996-1944/12/6/952#citedby) | Viewed by 1874

Open Access Article



./1996-1944/12/6/951/pdf)



Coupling Effect of Porosity and Cell Size on the Deformation Behavior of Al Alloy Foam under Quasi-Static Compression (/1996-1944/12/6/951)

Materials **2019**, *12*(6), 951; <https://doi.org/10.3390/ma12060951>

(<https://doi.org/10.3390/ma12060951>) - 21 Mar 2019

Cited by 5 (/1996-1944/12/6/951#citedby) | Viewed by 1128




Open Access Article    [\(/1996-1944/12/6/950/pdf\)](#)

Tribological Behavior of TiC Particles Reinforced 316Lss Composite Fabricated Using Selective Laser Melting [\(/1996-1944/12/6/950\)](#)   

Materials **2019**, *12*(6), 950; <https://doi.org/10.3390/ma12060950>

<https://doi.org/10.3390/ma12060950> - 21 Mar 2019

Cited by 7 [\(/1996-1944/12/6/950#citedby\)](#) | Viewed by 956

Open Access Communication   [\(/1996-1944/12/6/949/pdf\)](#) 

Cationic Albumin Encapsulated DNA Origami for Enhanced Cellular Transfection and Stability [\(/1996-1944/12/6/949\)](#)

Materials **2019**, *12*(6), 949; <https://doi.org/10.3390/ma12060949>

<https://doi.org/10.3390/ma12060949> - 21 Mar 2019

Cited by 14 [\(/1996-1944/12/6/949#citedby\)](#) | Viewed by 1658


Open Access Article   [\(/1996-1944/12/6/948/pdf\)](#)

Properties of Dislocation Drag from Phonon Wind at Ambient Conditions [\(/1996-1944/12/6/948\)](#)

Materials **2019**, *12*(6), 948; <https://doi.org/10.3390/ma12060948>

<https://doi.org/10.3390/ma12060948> - 21 Mar 2019

Cited by 8 [\(/1996-1944/12/6/948#citedby\)](#) | Viewed by 902



Open Access Article   [\(/1996-1944/12/6/947/pdf\)](#)

Optical Coherence Tomography Investigations and Modeling of the Sintering of Ceramic Crowns [\(/1996-1944/12/6/947\)](#)

Materials **2019**, *12*(6), 947; <https://doi.org/10.3390/ma12060947>

<https://doi.org/10.3390/ma12060947> - 21 Mar 2019

Cited by 6 [\(/1996-1944/12/6/947#citedby\)](#) | Viewed by 1454



Open Access Article   [\(/1996-1944/12/6/946/pdf\)](#)

Microstructural Characterization of Porous Clay-Based Ceramic Composites [\(/1996-1944/12/6/946\)](#)

Materials **2019**, *12*(6), 946; <https://doi.org/10.3390/ma12060946>

<https://doi.org/10.3390/ma12060946> - 21 Mar 2019

Cited by 2 [\(/1996-1944/12/6/946#citedby\)](#) | Viewed by 1125

Open Access Article   [\(/1996-1944/12/6/945/pdf\)](#) 

Holographic Performance of Azo-Carbazole Dye-Doped UP Resin Films Using a Dyeing Process [\(/1996-1944/12/6/945\)](#)

Materials **2019**, *12*(6), 945; <https://doi.org/10.3390/ma12060945>

<https://doi.org/10.3390/ma12060945> - 21 Mar 2019

Cited by 1 [\(/1996-1944/12/6/945#citedby\)](#) | Viewed by 1326

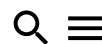
Open Access Article   [\(/1996-1944/12/6/944/pdf\)](#)

Investigation of Structural Degradation of Fiber Cement Boards Due to Thermal Impact (/1996-1944/12/6/944)

Materials 2019, 12(6), 944; <https://doi.org/10.3390/ma12060944>

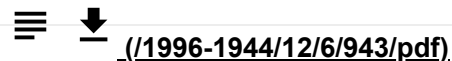
(<https://doi.org/10.3390/ma12060944>) - 21 Mar 2019

 [\(/toggle desktop layout cookie\)](#)



Cited by 11 (/1996-1944/12/6/944#citedby) | Viewed by 1185

Open Access Article



[\(/1996-1944/12/6/943/pdf\)](#)

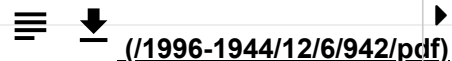
Investigation of the Influence of Reduced Graphene Oxide Flakes in the Dielectric on Surface Characteristics and Material Removal Rate in EDM (/1996-1944/12/6/943)

Materials 2019, 12(6), 943; <https://doi.org/10.3390/ma12060943>

(<https://doi.org/10.3390/ma12060943>) - 21 Mar 2019

Cited by 11 (/1996-1944/12/6/943#citedby) | Viewed by 895

Open Access Article



[\(/1996-1944/12/6/942/pdf\)](#)

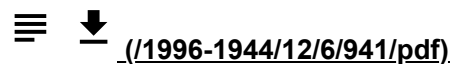
Fabrication of Carboxymethylcellulose/Metal-Organic Framework Beads for Removal of Pb(II) from Aqueous Solution (/1996-1944/12/6/942)

Materials 2019, 12(6), 942; <https://doi.org/10.3390/ma12060942>

(<https://doi.org/10.3390/ma12060942>) - 21 Mar 2019

Cited by 11 (/1996-1944/12/6/942#citedby) | Viewed by 1236

Open Access Article



[\(/1996-1944/12/6/941/pdf\)](#)

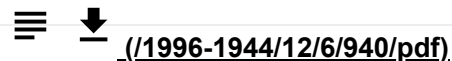
Evaluation of Properties and Microstructure of Cement Paste Blended with Metakaolin Subjected to High Temperatures (/1996-1944/12/6/941)

Materials 2019, 12(6), 941; <https://doi.org/10.3390/ma12060941>

(<https://doi.org/10.3390/ma12060941>) - 21 Mar 2019

Cited by 12 (/1996-1944/12/6/941#citedby) | Viewed by 986

Open Access Article



[\(/1996-1944/12/6/940/pdf\)](#)

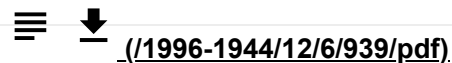
Corrosion Initiation and Propagation on Carburized Martensitic Stainless Steel Surfaces Studied via Advanced Scanning Probe Microscopy (/1996-1944/12/6/940)

Materials 2019, 12(6), 940; <https://doi.org/10.3390/ma12060940>

(<https://doi.org/10.3390/ma12060940>) - 21 Mar 2019

Cited by 4 (/1996-1944/12/6/940#citedby) | Viewed by 1219

Open Access Article



[\(/1996-1944/12/6/939/pdf\)](#)

Model Based on an Effective Material-Removal Rate to Evaluate Specific Energy Consumption in Grinding (/1996-1944/12/6/939)

Materials 2019, 12(6), 939; <https://doi.org/10.3390/ma12060939>

(<https://doi.org/10.3390/ma12060939>) - 21 Mar 2019

Cited by 1 (/1996-1944/12/6/939#citedby) | Viewed by 982

Open Access Article



[\(/1996-1944/12/6/938/pdf\)](#)

Enhancing Damage-Sensing Capacity of Strain-Hardening Macro-Steel Fiber-Reinforced Concrete by Adding Low Amount of Discrete Carbons (/1996-1944/12/6/938)

Materials 2019, 12(6), 938; <https://doi.org/10.3390/ma12060938>

(<https://doi.org/10.3390/ma12060938>) - 21 Mar 2019

Cited by 7 (</1996-1944/12/6/938#citedby>) | Viewed by 846

Open Access Article

Application of Reverse Micelle Sol–Gel Synthesis for Bulk Doping and Heteroatoms Surface Enrichment in Mo-Doped TiO₂ Nanoparticles (</1996-1944/12/6/937>)

Materials 2019, 12(6), 937; <https://doi.org/10.3390/ma12060937>

(<https://doi.org/10.3390/ma12060937>) - 21 Mar 2019

Cited by 5 (</1996-1944/12/6/937#citedby>) | Viewed by 1285

Open Access Article

Suppression of the Growth of Intermetallic Compound Layers with the Addition of Graphene Nano-Sheets to an Epoxy Sn–Ag–Cu Solder on a Cu Substrate (</1996-1944/12/6/936>)

Materials 2019, 12(6), 936; <https://doi.org/10.3390/ma12060936>

(<https://doi.org/10.3390/ma12060936>) - 21 Mar 2019

Cited by 2 (</1996-1944/12/6/936#citedby>) | Viewed by 1228

Open Access Article

Application of Inner Radiation Baffles in the Bridgman Process for Flattening the Temperature Profile and Controlling the Columnar Grain Structure of Directionally Solidified Ni-Based Superalloys (</1996-1944/12/6/935>)

Materials 2019, 12(6), 935; <https://doi.org/10.3390/ma12060935>

(<https://doi.org/10.3390/ma12060935>) - 21 Mar 2019

Cited by 7 (</1996-1944/12/6/935#citedby>) | Viewed by 1353

Open Access Article

Rapid Fabrication of High-Performance CaO-Based Integral Ceramic Mould by Stereolithography and Non-Aqueous Gelcasting (</1996-1944/12/6/934>)

Materials 2019, 12(6), 934; <https://doi.org/10.3390/ma12060934>

(<https://doi.org/10.3390/ma12060934>) - 21 Mar 2019

Cited by 3 (</1996-1944/12/6/934#citedby>) | Viewed by 1196

Open Access Article

Luminescent Mesoporous Silica Nanohybrid Based on Drug Derivative Terbium Complex (</1996-1944/12/6/933>)

Materials 2019, 12(6), 933; <https://doi.org/10.3390/ma12060933>

(<https://doi.org/10.3390/ma12060933>) - 21 Mar 2019

Cited by 6 (</1996-1944/12/6/933#citedby>) | Viewed by 1733

Open Access Article

Reactivity and Hydration Property of Synthetic Air Quenched Slag with Different Chemical Compositions (</1996-1944/12/6/932>)


Materials 2019, 12(6), 932; <https://doi.org/10.3390/ma12060932>

(<https://doi.org/10.3390/ma12060932>) - 20 Mar 2019

Cited by 3 (</1996-1944/12/6/932#citedby>) | Viewed by 1259

 [\(/toggle desktop layout cookie\)](#)  

Open Access Article

 [\(/1996-1944/12/6/931/pdf\)](/1996-1944/12/6/931/pdf)

Characterization of SiC Ceramic Joints Brazed Using Au–Ni–Pd–Ti High-Temperature Filler Alloy
(/1996-1944/12/6/931)

Materials 2019, 12(6), 931; <https://doi.org/10.3390/ma12060931>

(<https://doi.org/10.3390/ma12060931>) - 20 Mar 2019

Cited by 1 (</1996-1944/12/6/931#citedby>) | Viewed by 1007

Open Access Article

 [\(/1996-1944/12/6/930/pdf\)](/1996-1944/12/6/930/pdf)

Effect of Process Parameters and High-Temperature Preheating on Residual Stress and Relative Density of Ti6Al4V Processed by Selective Laser Melting
(/1996-1944/12/6/930)

Materials 2019, 12(6), 930; <https://doi.org/10.3390/ma12060930>

(<https://doi.org/10.3390/ma12060930>) - 20 Mar 2019

Cited by 18 (</1996-1944/12/6/930#citedby>) | Viewed by 1704

Open Access Article

 [\(/1996-1944/12/6/929/pdf\)](/1996-1944/12/6/929/pdf)

Highly Selective CMOS-Compatible Mid-Infrared Thermal Emitter/Detector Slab Design Using Optical Tamm-States
(/1996-1944/12/6/929)

Materials 2019, 12(6), 929; <https://doi.org/10.3390/ma12060929>

(<https://doi.org/10.3390/ma12060929>) - 20 Mar 2019

Cited by 5 (</1996-1944/12/6/929#citedby>) | Viewed by 908

Open Access Article

 [\(/1996-1944/12/6/928/pdf\)](/1996-1944/12/6/928/pdf)

Magnetic Field Patterning of Nickel Nanowire Film Realized by Printed Precursor Inks
(/1996-1944/12/6/928)

Materials 2019, 12(6), 928; <https://doi.org/10.3390/ma12060928>

(<https://doi.org/10.3390/ma12060928>) - 20 Mar 2019

Cited by 1 (</1996-1944/12/6/928#citedby>) | Viewed by 1210

Open Access Review

 [\(/1996-1944/12/6/927/pdf\)](/1996-1944/12/6/927/pdf)


Removal of Hazardous Oxyanions from the Environment Using Metal-Oxide-Based Materials
(/1996-1944/12/6/927)

Materials 2019, 12(6), 927; <https://doi.org/10.3390/ma12060927>

(<https://doi.org/10.3390/ma12060927>) - 20 Mar 2019

Cited by 13 (</1996-1944/12/6/927#citedby>) | Viewed by 1562

Open Access Article

 [\(/1996-1944/12/6/926/pdf\)](/1996-1944/12/6/926/pdf)

Microstructure, Thermal, and Corrosion Behavior of the AlAgCuNiSnTi Equiatomic Multicomponent Alloy
(/1996-1944/12/6/926)

Materials 2019, 12(6), 926; <https://doi.org/10.3390/ma12060926>

(<https://doi.org/10.3390/ma12060926>) - 20 Mar 2019

Cited by 6 (</1996-1944/12/6/926#citedby>) | Viewed by 967



Open Access Article

[\(/1996-1944/12/6/925/pdf\)](/1996-1944/12/6/925/pdf)

Use of Ladle Furnace Slag and Other Industrial By-Products to Encapsulate Chloride in Municipal Solid Waste Incineration Fly Ash (/1996-1944/12/6/925)

Materials 2019, 12(6), 925; <https://doi.org/10.3390/ma12060925>

(<https://doi.org/10.3390/ma12060925>) - 20 Mar 2019

Cited by 2 (</1996-1944/12/6/925#citedby>) | Viewed by 1308

Open Access Article

[\(/1996-1944/12/6/924/pdf\)](/1996-1944/12/6/924/pdf)

Fast Removal of Propranolol from Water by Attapulgitte/Graphene Oxide Magnetic Ternary Composites (/1996-1944/12/6/924)

Materials 2019, 12(6), 924; <https://doi.org/10.3390/ma12060924>

(<https://doi.org/10.3390/ma12060924>) - 20 Mar 2019

Cited by 5 (</1996-1944/12/6/924#citedby>) | Viewed by 921

Open Access Article

[\(/1996-1944/12/6/923/pdf\)](/1996-1944/12/6/923/pdf)

Ambient Cured Fly Ash Geopolymer Coatings for Concrete (/1996-1944/12/6/923)

Materials 2019, 12(6), 923; <https://doi.org/10.3390/ma12060923>

(<https://doi.org/10.3390/ma12060923>) - 20 Mar 2019

Cited by 20 (</1996-1944/12/6/923#citedby>) | Viewed by 1510

Open Access Article

[\(/1996-1944/12/6/922/pdf\)](/1996-1944/12/6/922/pdf)

Effect of Hot-Pressing Temperature on Characteristics of Straw-Based Binderless Fiberboards with Pulping Effluent (/1996-1944/12/6/922)

Materials 2019, 12(6), 922; <https://doi.org/10.3390/ma12060922>

(<https://doi.org/10.3390/ma12060922>) - 20 Mar 2019

Cited by 2 (</1996-1944/12/6/922#citedby>) | Viewed by 910

Open Access Article

[\(/1996-1944/12/6/921/pdf\)](/1996-1944/12/6/921/pdf)

Physical, Chemical, Microstructural and Rheological Properties of Reactive Terpolymer-Modified Bitumen (/1996-1944/12/6/921)

Materials 2019, 12(6), 921; <https://doi.org/10.3390/ma12060921>

(<https://doi.org/10.3390/ma12060921>) - 20 Mar 2019

Cited by 5 (</1996-1944/12/6/921#citedby>) | Viewed by 1212

Open Access Article

[\(/1996-1944/12/6/920/pdf\)](/1996-1944/12/6/920/pdf)

Tribological Characterization of Micron-/Nano-Sized WC-9%Co Cemented Carbides Prepared by Spark Plasma Sintering at Elevated Temperatures (/1996-1944/12/6/920)

Materials 2019, 12(6), 920; <https://doi.org/10.3390/ma12060920>

(<https://doi.org/10.3390/ma12060920>) - 20 Mar 2019

Cited by 6 (/1996-1944/12/6/920#citedby) | Viewed by 1223

MDPI

Open Access Feature Paper Article



(/1996-1944/12/6/919/pdf)

Bone Tissue Engineering in a Perfusion Bioreactor Using Dexamethasone-Loaded Peptide Hydrogel (/1996-1944/12/6/919)

Materials **2019**, *12*(6), 919; <https://doi.org/10.3390/ma12060919>

(<https://doi.org/10.3390/ma12060919>) - 19 Mar 2019

Cited by 2 (/1996-1944/12/6/919#citedby) | Viewed by 1664

Open Access Article



(/1996-1944/12/6/918/pdf)

The Study of Buckling and Post-Buckling of a Step-Variable FGM Box (/1996-1944/12/6/918)

Materials **2019**, *12*(6), 918; <https://doi.org/10.3390/ma12060918>

(<https://doi.org/10.3390/ma12060918>) - 19 Mar 2019

Cited by 4 (/1996-1944/12/6/918#citedby) | Viewed by 791

Open Access Article



(/1996-1944/12/6/917/pdf)

Database of Shear Experiments on Steel Fiber Reinforced Concrete Beams without Stirrups (/1996-1944/12/6/917)

Materials **2019**, *12*(6), 917; <https://doi.org/10.3390/ma12060917>

(<https://doi.org/10.3390/ma12060917>) - 19 Mar 2019

Cited by 18 (/1996-1944/12/6/917#citedby) | Viewed by 1902

Open Access Article



(/1996-1944/12/6/916/pdf)

Mechanical and Cytocompatibility Evaluation of UHMWPE/PCL/Bioglass® Fibrous Composite for Acetabular Labrum Implant (/1996-1944/12/6/916)

Materials **2019**, *12*(6), 916; <https://doi.org/10.3390/ma12060916>

(<https://doi.org/10.3390/ma12060916>) - 19 Mar 2019

Cited by 4 (/1996-1944/12/6/916#citedby) | Viewed by 1039

Open Access Article



(/1996-1944/12/6/915/pdf)

Advantages of the Application of the Temper Bead Welding Technique During Wet Welding (/1996-1944/12/6/915)

Materials **2019**, *12*(6), 915; <https://doi.org/10.3390/ma12060915>

(<https://doi.org/10.3390/ma12060915>) - 19 Mar 2019

Cited by 22 (/1996-1944/12/6/915#citedby) | Viewed by 2430

Open Access Article



(/1996-1944/12/6/914/pdf)



Oxidation Resistance and Microstructure Evaluation of a Polymer Derived Ceramic (PDC) Composite Coating Applied onto Sintered Steel (/1996-1944/12/6/914)


Materials **2019**, *12*(6), 914; <https://doi.org/10.3390/ma12060914>

(<https://doi.org/10.3390/ma12060914>) - 19 Mar 2019

Cited by 2 (/1996-1944/12/6/914#citedby) | Viewed by 1069



Open Access Article

  [\(/1996-1944/12/6/913/pdf\)](#)

Parametric Modeling of Biomimetic Cortical Bone Microstructure for Additive Manufacturing
(/1996-1944/12/6/913)



  [\(/toggle_desktop_layout_cookie\)](#)  

Materials **2019**, *12*(6), 913; <https://doi.org/10.3390/ma12060913>

[\(/1996-1944/12/6/913\)](https://doi.org/10.3390/ma12060913) - 19 Mar 2019

Cited by 6 [\(/1996-1944/12/6/913#citedby\)](#) | Viewed by 2347

Open Access Article

  [\(/1996-1944/12/6/912/pdf\)](#)

Evaluation and Selection of De-Icing Salt Based on Multi-Factor
(/1996-1944/12/6/912)

Materials **2019**, *12*(6), 912; <https://doi.org/10.3390/ma12060912>

[\(/1996-1944/12/6/912\)](https://doi.org/10.3390/ma12060912) - 19 Mar 2019

Cited by 1 [\(/1996-1944/12/6/912#citedby\)](#) | Viewed by 1070

Open Access Feature Paper Article

  [\(/1996-1944/12/6/911/pdf\)](#)

Room Temperature Synthesis of V-Doped TiO₂ and Its Photocatalytic Activity in the Removal of Caffeine under UV Irradiation
(/1996-1944/12/6/911)

Materials **2019**, *12*(6), 911; <https://doi.org/10.3390/ma12060911>

[\(/1996-1944/12/6/911\)](https://doi.org/10.3390/ma12060911) - 19 Mar 2019

Cited by 11 [\(/1996-1944/12/6/911#citedby\)](#) | Viewed by 1040

Open Access Article

  [\(/1996-1944/12/6/910/pdf\)](#)

Binary Oxides Prepared by Microwave-Assisted Solution Combustion: Synthesis, Characterization and Catalytic Activity
(/1996-1944/12/6/910)

Materials **2019**, *12*(6), 910; <https://doi.org/10.3390/ma12060910>

[\(/1996-1944/12/6/910\)](https://doi.org/10.3390/ma12060910) - 19 Mar 2019

Cited by 3 [\(/1996-1944/12/6/910#citedby\)](#) | Viewed by 1317

Open Access Article

  [\(/1996-1944/12/6/909/pdf\)](#)

Nanocomplexes of Graphene Oxide and Platinum Nanoparticles against Colorectal Cancer Colo205, HT-29, HTC-116, SW480, Liver Cancer HepG2, Human Breast Cancer MCF-7, and Adenocarcinoma LNCaP and Human Cervical Hela B Cell Lines
(/1996-1944/12/6/909)

Materials **2019**, *12*(6), 909; <https://doi.org/10.3390/ma12060909>

[\(/1996-1944/12/6/909\)](https://doi.org/10.3390/ma12060909) - 19 Mar 2019

Cited by 8 [\(/1996-1944/12/6/909#citedby\)](#) | Viewed by 1679

Open Access Feature Paper Review

  [\(/1996-1944/12/6/908/pdf\)](#)

Regenerative Endodontic Procedures Using Contemporary Endodontic Materials
(/1996-1944/12/6/908)

Materials **2019**, *12*(6), 908; <https://doi.org/10.3390/ma12060908>

[\(/1996-1944/12/6/908\)](https://doi.org/10.3390/ma12060908) - 19 Mar 2019

Cited by 12 [\(/1996-1944/12/6/908#citedby\)](#) | Viewed by 2894

Open Access Review

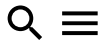
  [\(/1996-1944/12/6/907/pdf\)](#)

Advanced Electric Discharge Machining of Stainless Steels: Assessment of the State of the Art, Gaps and Future Prospect (/1996-1944/12/6/907)

Materials 2019, 12(6), 907; <https://doi.org/10.3390/ma12060907>

(<https://doi.org/10.3390/ma12060907>) - 19 Mar 2019

 [\(/toggle desktop layout cookie\)](#)



Cited by 28 (/1996-1944/12/6/907#citedby) | Viewed by 1890

Open Access Article



[\(/1996-1944/12/6/906/pdf\)](#)

Prototype Orthopedic Bone Plates 3D Printed by Laser Melting Deposition (/1996-1944/12/6/906)

Materials 2019, 12(6), 906; <https://doi.org/10.3390/ma12060906>

(<https://doi.org/10.3390/ma12060906>) - 19 Mar 2019

Cited by 7 (/1996-1944/12/6/906#citedby) | Viewed by 1431

Open Access Article



[\(/1996-1944/12/6/905/pdf\)](#)

Construction Materials from Vitrified Lignite Fly Ash in Plasmatron Plasma Reactor (/1996-1944/12/6/905)

Materials 2019, 12(6), 905; <https://doi.org/10.3390/ma12060905>

(<https://doi.org/10.3390/ma12060905>) - 19 Mar 2019

Cited by 3 (/1996-1944/12/6/905#citedby) | Viewed by 1019

Open Access Article



[\(/1996-1944/12/6/904/pdf\)](#)



Peptide Controlled Shaping of Biomineralized Tin(II) Oxide into Flower-Like Particles (/1996-1944/12/6/904)

Materials 2019, 12(6), 904; <https://doi.org/10.3390/ma12060904>

(<https://doi.org/10.3390/ma12060904>) - 18 Mar 2019

Cited by 1 (/1996-1944/12/6/904#citedby) | Viewed by 1361

Open Access Article



[\(/1996-1944/12/6/903/pdf\)](#)

Tribological Properties of Molybdenum Disulfide and Helical Carbon Nanotube Modified Epoxy Resin (/1996-1944/12/6/903)

Materials 2019, 12(6), 903; <https://doi.org/10.3390/ma12060903>

(<https://doi.org/10.3390/ma12060903>) - 18 Mar 2019

Cited by 5 (/1996-1944/12/6/903#citedby) | Viewed by 1162

Open Access Article



[\(/1996-1944/12/6/902/pdf\)](#)

Method of Optimisation for Ambient Temperature Cured Sustainable Geopolymers for 3D Printing Construction Applications (/1996-1944/12/6/902)

Materials 2019, 12(6), 902; <https://doi.org/10.3390/ma12060902>

(<https://doi.org/10.3390/ma12060902>) - 18 Mar 2019

Cited by 26 (/1996-1944/12/6/902#citedby) | Viewed by 1760

Open Access Article



[\(/1996-1944/12/6/901/pdf\)](#)

Synthesis of Nanocrystalline AZ91 Magnesium Alloy Dispersed with 15 vol.% Submicron SiC Particles by Mechanical Milling (/1996-1944/12/6/901)


Materials 2019, 12(6), 901; <https://doi.org/10.3390/ma12060901>

(<https://doi.org/10.3390/ma12060901>) - 18 Mar 2019

Cited by 1 (</1996-1944/12/6/901#citedby>) | Viewed by 1005

 [\(/toggle desktop layout cookie\)](#)  

Open Access Article

 [\(/1996-1944/12/6/900/pdf\)](/1996-1944/12/6/900/pdf)

Correlation of Macroscopic Fracture Behavior with Microscopic Fracture Mechanism for AHSS Sheet (</1996-1944/12/6/900>)

Materials 2019, 12(6), 900; <https://doi.org/10.3390/ma12060900>

(<https://doi.org/10.3390/ma12060900>) - 18 Mar 2019

Cited by 3 (</1996-1944/12/6/900#citedby>) | Viewed by 910

Open Access Article

 [\(/1996-1944/12/6/899/pdf\)](/1996-1944/12/6/899/pdf)


Study on the Properties of Vertical Carbon Nanotube Films Grown on Stainless Steel Bipolar Plates (</1996-1944/12/6/899>)

Materials 2019, 12(6), 899; <https://doi.org/10.3390/ma12060899>

(<https://doi.org/10.3390/ma12060899>) - 18 Mar 2019

Cited by 5 (</1996-1944/12/6/899#citedby>) | Viewed by 1110

Open Access Article

 [\(/1996-1944/12/6/898/pdf\)](/1996-1944/12/6/898/pdf)

Tuning Optical and Granulometric Properties of Gold Nanostructures Synthesized with the Aid of Different Types of Honeys for Microwave-Induced Hyperthermia (</1996-1944/12/6/898>)

Materials 2019, 12(6), 898; <https://doi.org/10.3390/ma12060898>

(<https://doi.org/10.3390/ma12060898>) - 18 Mar 2019

Viewed by 892

Open Access Article

 [\(/1996-1944/12/6/897/pdf\)](/1996-1944/12/6/897/pdf)


Porous Alumina Ceramics Obtained by Particles Self-Assembly Combining Freeze Drying Method (</1996-1944/12/6/897>)

Materials 2019, 12(6), 897; <https://doi.org/10.3390/ma12060897>

(<https://doi.org/10.3390/ma12060897>) - 18 Mar 2019

Cited by 1 (</1996-1944/12/6/897#citedby>) | Viewed by 996

Open Access Article

 [\(/1996-1944/12/6/896/pdf\)](/1996-1944/12/6/896/pdf)


Preparation of PAN@TiO₂ Nanofibers for Fruit Packaging Materials with Efficient Photocatalytic Degradation of Ethylene (</1996-1944/12/6/896>)

Materials 2019, 12(6), 896; <https://doi.org/10.3390/ma12060896>

(<https://doi.org/10.3390/ma12060896>) - 18 Mar 2019

Cited by 10 (</1996-1944/12/6/896#citedby>) | Viewed by 1208

Open Access Review

 [\(/1996-1944/12/6/895/pdf\)](/1996-1944/12/6/895/pdf)

Characterization of the Mechanical Properties of FFF Structures and Materials: A Review on the Experimental, Computational and Theoretical Approaches (</1996-1944/12/6/895>)

Materials **2019**, 12(6), 895; <https://doi.org/10.3390/ma12060895>

(<https://doi.org/10.3390/ma12060895>) - 18 Mar 2019

Cited by 42 (</1996-1944/12/6/895#citedby>) | Viewed by 2453

Open Access Article

Noble Metal Composite Porous Silk Fibroin Aerogel Fibers (</1996-1944/12/6/894>)

Materials **2019**, 12(6), 894; <https://doi.org/10.3390/ma12060894>

(<https://doi.org/10.3390/ma12060894>) - 18 Mar 2019

Cited by 6 (</1996-1944/12/6/894#citedby>) | Viewed by 1584

Open Access Article

Ultrasonic Modification of Ag Nanowires and Their Applications in Flexible Transparent Film Heaters and SERS Detectors (</1996-1944/12/6/893>)

Materials **2019**, 12(6), 893; <https://doi.org/10.3390/ma12060893>

(<https://doi.org/10.3390/ma12060893>) - 18 Mar 2019

Cited by 1 (</1996-1944/12/6/893#citedby>) | Viewed by 1207

Open Access Article

Modeling of Magnetorheological Elastomers Using the Elastic–Plastic Model with Kinematic Hardening (</1996-1944/12/6/892>)

Materials **2019**, 12(6), 892; <https://doi.org/10.3390/ma12060892>

(<https://doi.org/10.3390/ma12060892>) - 18 Mar 2019

Cited by 4 (</1996-1944/12/6/892#citedby>) | Viewed by 992

Open Access Feature Paper Article

Evaluation of Joint Formation and Mechanical Performance of the AA7075-T6/CFRP Spot Joints Produced by Frictional Heat (</1996-1944/12/6/891>)

Materials **2019**, 12(6), 891; <https://doi.org/10.3390/ma12060891>

(<https://doi.org/10.3390/ma12060891>) - 17 Mar 2019

Cited by 5 (</1996-1944/12/6/891#citedby>) | Viewed by 1189

Open Access Article

Crack Healing and Mechanical Properties Recovery in SA 508–3 Steel (</1996-1944/12/6/890>)

Materials **2019**, 12(6), 890; <https://doi.org/10.3390/ma12060890>

(<https://doi.org/10.3390/ma12060890>) - 17 Mar 2019

Cited by 5 (</1996-1944/12/6/890#citedby>) | Viewed by 976

Open Access Article

Unified Strength Model of Asphalt Mixture under Various Loading Modes (</1996-1944/12/6/889>)

Materials **2019**, 12(6), 889; <https://doi.org/10.3390/ma12060889>

(<https://doi.org/10.3390/ma12060889>) - 17 Mar 2019

Cited by 5 (</1996-1944/12/6/889#citedby>) | Viewed by 1215 | [Correction \(</1996-1944/13/23/5393>\)](/1996-1944/13/23/5393)

Open Access Article

[\(/1996-1944/12/6/888/pdf\)](#)

ZnCr₂O₄ Inclusions in ZnO Matrix Investigated by Probe-Corrected STEM-EELS (/1996-1944/12/6/888)

Materials **2019**, *12*(6), 888; <https://doi.org/10.3390/ma12060888>

(<https://doi.org/10.3390/ma12060888>) - 16 Mar 2019

Viewed by 1916

Open Access Article

[\(/1996-1944/12/6/887/pdf\)](#)

Medical-Grade PCL Based Polyurethane System for FDM 3D Printing—Characterization and Fabrication (/1996-1944/12/6/887)

Materials **2019**, *12*(6), 887; <https://doi.org/10.3390/ma12060887>

(<https://doi.org/10.3390/ma12060887>) - 16 Mar 2019

Cited by 23 ([/1996-1944/12/6/887#citedby](#)) | Viewed by 2696

Open Access Article

[\(/1996-1944/12/6/886/pdf\)](#)

Identification of Mechanical Properties for Titanium Alloy Ti-6Al-4V Produced Using LENS Technology (/1996-1944/12/6/886)

Materials **2019**, *12*(6), 886; <https://doi.org/10.3390/ma12060886>

(<https://doi.org/10.3390/ma12060886>) - 16 Mar 2019

Cited by 12 ([/1996-1944/12/6/886#citedby](#)) | Viewed by 1324

Open Access Article

[\(/1996-1944/12/6/885/pdf\)](#)

Visual Appearance of Nanocrystal-Based Luminescent Solar Concentrators (/1996-1944/12/6/885)

Materials **2019**, *12*(6), 885; <https://doi.org/10.3390/ma12060885>

(<https://doi.org/10.3390/ma12060885>) - 16 Mar 2019

Cited by 4 ([/1996-1944/12/6/885#citedby](#)) | Viewed by 1813

Open Access Article

[\(/1996-1944/12/6/884/pdf\)](#)

Structured Monolithic Catalysts vs. Fixed Bed for the Oxidative Dehydrogenation of Propane (/1996-1944/12/6/884)

Materials **2019**, *12*(6), 884; <https://doi.org/10.3390/ma12060884>

(<https://doi.org/10.3390/ma12060884>) - 16 Mar 2019

Cited by 2 ([/1996-1944/12/6/884#citedby](#)) | Viewed by 1098

Open Access Article

[\(/1996-1944/12/6/883/pdf\)](#)

Experimental and Numerical Investigation of Mechanical and Thermal Effects in TiNi SMA during Transformation-Induced Creep Phenomena (/1996-1944/12/6/883)

Materials **2019**, *12*(6), 883; <https://doi.org/10.3390/ma12060883>

(<https://doi.org/10.3390/ma12060883>) - 16 Mar 2019

Cited by 1 ([/1996-1944/12/6/883#citedby](#)) | Viewed by 1020

Open Access Article

[\(/1996-1944/12/6/882/pdf\)](#)



Preparation of Sludge-Derived Activated Carbon by Fenton Activation and the Adsorption of Eriochrome Black T (/1996-1944/12/6/882)

Materials 2019, 12(6), 882; <https://doi.org/10.3390/ma12060882>

(<https://doi.org/10.3390/ma12060882>) - 16 Mar 2019

Cited by 4 (</1996-1944/12/6/882#citedby>) | Viewed by 1267

Open Access Article

  [_\(/1996-1944/12/6/881/pdf\)](/1996-1944/12/6/881/pdf)

Thermal Properties of Wood-Plastic Composites with Different Compositions (/1996-1944/12/6/881)

Materials 2019, 12(6), 881; <https://doi.org/10.3390/ma12060881>

(<https://doi.org/10.3390/ma12060881>) - 15 Mar 2019

Cited by 8 (</1996-1944/12/6/881#citedby>) | Viewed by 1345

Open Access Article

  [_\(/1996-1944/12/6/880/pdf\)](/1996-1944/12/6/880/pdf)



Modification of Pyrolytic Oil from Waste Tyres as a Promising Method for Light Fuel Production (/1996-1944/12/6/880)

Materials 2019, 12(6), 880; <https://doi.org/10.3390/ma12060880>

(<https://doi.org/10.3390/ma12060880>) - 15 Mar 2019

Cited by 7 (</1996-1944/12/6/880#citedby>) | Viewed by 963

Open Access Article

  [_\(/1996-1944/12/6/879/pdf\)](/1996-1944/12/6/879/pdf)


Intelligent Optimization of Hard-Turning Parameters Using Evolutionary Algorithms for Smart Manufacturing (/1996-1944/12/6/879)

Materials 2019, 12(6), 879; <https://doi.org/10.3390/ma12060879>

(<https://doi.org/10.3390/ma12060879>) - 15 Mar 2019

Cited by 34 (</1996-1944/12/6/879#citedby>) | Viewed by 1396

Open Access Article

  [_\(/1996-1944/12/6/878/pdf\)](/1996-1944/12/6/878/pdf)




Combustion Synthesis of Non-Precious CuO-CeO₂ Nanocrystalline Catalysts with Enhanced Catalytic Activity for Methane Oxidation (/1996-1944/12/6/878)

Materials 2019, 12(6), 878; <https://doi.org/10.3390/ma12060878>

(<https://doi.org/10.3390/ma12060878>) - 15 Mar 2019

Cited by 9 (</1996-1944/12/6/878#citedby>) | Viewed by 1150

Open Access Article

  [_\(/1996-1944/12/6/877/pdf\)](/1996-1944/12/6/877/pdf) 


Metal Oxide Thin Films Prepared by Magnetron Sputtering Technology for Volatile Organic Compound Detection in the Microwave Frequency Range (/1996-1944/12/6/877)

Materials 2019, 12(6), 877; <https://doi.org/10.3390/ma12060877>

(<https://doi.org/10.3390/ma12060877>) - 15 Mar 2019

Cited by 15 (</1996-1944/12/6/877#citedby>) | Viewed by 1443

Open Access Article

  [_\(/1996-1944/12/6/876/pdf\)](/1996-1944/12/6/876/pdf)

A Comprehensive Study on The Accelerated Weathering Properties of Polypropylene—Wood Composites with Non-Metallic Materials of Waste-Printed Circuit Board Powders (/1996-

1944/12/6/876).

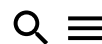
 *Materials* **2019**, *12*(6), 876; <https://doi.org/10.3390/ma12060876>

(<https://doi.org/10.3390/ma12060876>) - 15 Mar 2019

Cited by 5 (</1996-1944/12/6/876#citedby>) | Viewed by 924



[\(/toggle_desktop_layout_cookie\)](#)



Open Access Article



[\(/1996-1944/12/6/875/pdf\)](#)

Memristor-CMOS Hybrid Circuit for Temporal-Pooling of Sensory and Hippocampal Responses of Cortical Neurons (</1996-1944/12/6/875>)

Materials **2019**, *12*(6), 875; <https://doi.org/10.3390/ma12060875>

(<https://doi.org/10.3390/ma12060875>) - 15 Mar 2019

Cited by 3 (</1996-1944/12/6/875#citedby>) | Viewed by 1322

Open Access Article



[\(/1996-1944/12/6/874/pdf\)](#)

Dealing with Nap-Core Sandwich Composites: How to Predict the Effect of Symmetry (</1996-1944/12/6/874>)

Materials **2019**, *12*(6), 874; <https://doi.org/10.3390/ma12060874>

(<https://doi.org/10.3390/ma12060874>) - 15 Mar 2019

Cited by 1 (</1996-1944/12/6/874#citedby>) | Viewed by 1161

Open Access Feature Paper Article



[\(/1996-1944/12/6/873/pdf\)](#)

Photocatalytic Degradation of Azithromycin by Nanostructured TiO₂ Film: Kinetics, Degradation Products, and Toxicity (</1996-1944/12/6/873>)

Materials **2019**, *12*(6), 873; <https://doi.org/10.3390/ma12060873>

(<https://doi.org/10.3390/ma12060873>) - 15 Mar 2019

Cited by 7 (</1996-1944/12/6/873#citedby>) | Viewed by 1498

Open Access Article



[\(/1996-1944/12/6/872/pdf\)](#)

Strain Rate during Creep in High-Pressure Die-Cast AZ91 Magnesium Alloys at Intermediate Temperatures (</1996-1944/12/6/872>)

Materials **2019**, *12*(6), 872; <https://doi.org/10.3390/ma12060872>

(<https://doi.org/10.3390/ma12060872>) - 15 Mar 2019

Viewed by 1051

Open Access Feature Paper Article



[\(/1996-1944/12/6/871/pdf\)](#)

Influence of Manufacturing Parameters on Mechanical Properties of Porous Materials by Selective Laser Sintering (</1996-1944/12/6/871>)

Materials **2019**, *12*(6), 871; <https://doi.org/10.3390/ma12060871>

(<https://doi.org/10.3390/ma12060871>) - 15 Mar 2019

Cited by 15 (</1996-1944/12/6/871#citedby>) | Viewed by 1417

Open Access Article



[\(/1996-1944/12/6/870/pdf\)](#)

Defect Creation in the Root of Single-Crystalline Turbine Blades Made of Ni-Based Superalloy (</1996-1944/12/6/870>)

Materials 2019, 12(6), 870; <https://doi.org/10.3390/ma12060870>

(<https://doi.org/10.3390/ma12060870>) - 15 Mar 2019

Cited by 3 (</1996-1944/12/6/870#citedby>) | Viewed by 1034

 
[\(/toggle_desktop_layout_cookie\)](#)

Open Access Article

[./1996-1944/12/6/869/pdf](/1996-1944/12/6/869/pdf)

Multifunctional Performance of a Nano-Modified Fiber Reinforced Composite Aeronautical Panel
(/1996-1944/12/6/869)

Materials 2019, 12(6), 869; <https://doi.org/10.3390/ma12060869>

(<https://doi.org/10.3390/ma12060869>) - 15 Mar 2019

Cited by 13 (</1996-1944/12/6/869#citedby>) | Viewed by 1161

Open Access Feature Paper Article

 
[./1996-1944/12/6/868/pdf](/1996-1944/12/6/868/pdf) 



Unsaturated Poly(Hydroxyalkanoates) for the Production of Nanoparticles and the Effect of
Cross-Linking on Nanoparticle Features (</1996-1944/12/6/868>)

Materials 2019, 12(6), 868; <https://doi.org/10.3390/ma12060868>

(<https://doi.org/10.3390/ma12060868>) - 15 Mar 2019

Cited by 4 (</1996-1944/12/6/868#citedby>) | Viewed by 892

Open Access Article

 
[./1996-1944/12/6/867/pdf](/1996-1944/12/6/867/pdf)



Magnetostrictive Guided Wave Technique Verification for Detection and Monitoring Defects in the
Pipe Weld (</1996-1944/12/6/867>)

Materials 2019, 12(6), 867; <https://doi.org/10.3390/ma12060867>

(<https://doi.org/10.3390/ma12060867>) - 15 Mar 2019

Cited by 3 (</1996-1944/12/6/867#citedby>) | Viewed by 948

Open Access Article

 
[./1996-1944/12/6/866/pdf](/1996-1944/12/6/866/pdf)



Bactericidal and Biocompatible Properties of Plasma Chemical Oxidized Titanium (TiOB[®]) with
Antimicrobial Surface Functionalization (</1996-1944/12/6/866>)

Materials 2019, 12(6), 866; <https://doi.org/10.3390/ma12060866>

(<https://doi.org/10.3390/ma12060866>) - 15 Mar 2019

Cited by 3 (</1996-1944/12/6/866#citedby>) | Viewed by 1285

Open Access Article

 
[./1996-1944/12/6/865/pdf](/1996-1944/12/6/865/pdf)



Effect by Diamond Surface Modification on Biomolecular Adhesion (</1996-1944/12/6/865>)

Materials 2019, 12(6), 865; <https://doi.org/10.3390/ma12060865>

(<https://doi.org/10.3390/ma12060865>) - 15 Mar 2019

Cited by 2 (</1996-1944/12/6/865#citedby>) | Viewed by 1082

Open Access Feature Paper Article

 
[./1996-1944/12/6/864/pdf](/1996-1944/12/6/864/pdf)

Microstructure and Mechanical Performance of Additively Manufactured Aluminum 2024-
T3/Acrylonitrile Butadiene Styrene Hybrid Joints Using an AddJoining Technique (</1996-1944/12/6/864>)

Materials 2019, 12(6), 864; <https://doi.org/10.3390/ma12060864>

(<https://doi.org/10.3390/ma12060864>) - 14 Mar 2019

Cited by 5 (</1996-1944/12/6/864#citedby>) | Viewed by 1410

[Correction \(/1996-1944/13/6/1460\)](/1996-1944/13/6/1460)

[\(/toggle desktop layout cookie\)](#)

Open Access Article

[\(/1996-1944/12/6/863/pdf\)](/1996-1944/12/6/863/pdf)

Effects of Finish Line Design and Fatigue Cyclic Loading on Phase Transformation of Zirconia Dental Ceramics: A Qualitative Micro-Raman Spectroscopic Analysis (</1996-1944/12/6/863>)

Materials 2019, 12(6), 863; <https://doi.org/10.3390/ma12060863>

(<https://doi.org/10.3390/ma12060863>) - 14 Mar 2019

Cited by 5 (</1996-1944/12/6/863#citedby>) | Viewed by 1318

Open Access Article

[\(/1996-1944/12/6/862/pdf\)](/1996-1944/12/6/862/pdf)

Rebar Corrosion Investigation in Rubber Aggregate Concrete via the Chloride Electro-Accelerated Test (</1996-1944/12/6/862>)

Materials 2019, 12(6), 862; <https://doi.org/10.3390/ma12060862>

(<https://doi.org/10.3390/ma12060862>) - 14 Mar 2019

Cited by 7 (</1996-1944/12/6/862#citedby>) | Viewed by 1024

Open Access Article

[\(/1996-1944/12/6/861/pdf\)](/1996-1944/12/6/861/pdf)

Hybrid Superconducting-Ferromagnetic $[\text{Bi}_2\text{Sr}_2(\text{Ca},\text{Y})_2\text{Cu}_3\text{O}_{10}]_{0.99}(\text{La}_{2/3}\text{Ba}_{1/3}\text{MnO}_3)_{0.01}$ Composite Thick Films (</1996-1944/12/6/861>)

Materials 2019, 12(6), 861; <https://doi.org/10.3390/ma12060861>

(<https://doi.org/10.3390/ma12060861>) - 14 Mar 2019

Cited by 2 (</1996-1944/12/6/861#citedby>) | Viewed by 843

Open Access Article

[\(/1996-1944/12/6/860/pdf\)](/1996-1944/12/6/860/pdf)

Optimal Machining Strategy Selection in Ball-End Milling of Hardened Steels for Injection Molds (</1996-1944/12/6/860>)

Materials 2019, 12(6), 860; <https://doi.org/10.3390/ma12060860>

(<https://doi.org/10.3390/ma12060860>) - 14 Mar 2019

Cited by 4 (</1996-1944/12/6/860#citedby>) | Viewed by 1007

Open Access Review

[\(/1996-1944/12/6/859/pdf\)](/1996-1944/12/6/859/pdf)

Inorganic and Hybrid Perovskite Based Laser Devices: A Review (</1996-1944/12/6/859>)

Materials 2019, 12(6), 859; <https://doi.org/10.3390/ma12060859>

(<https://doi.org/10.3390/ma12060859>) - 14 Mar 2019

Cited by 44 (</1996-1944/12/6/859#citedby>) | Viewed by 3102

Open Access Article

[\(/1996-1944/12/6/858/pdf\)](/1996-1944/12/6/858/pdf)

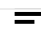

Using Green Supplementary Materials to Achieve More Ductile ECC (</1996-1944/12/6/858>)

Materials 2019, 12(6), 858; <https://doi.org/10.3390/ma12060858>

(<https://doi.org/10.3390/ma12060858>) - 14 Mar 2019

Cited by 11 (</1996-1944/12/6/858#citedby>) | Viewed by 1117

Open Access Article

  [\(/1996-1944/12/6/857/pdf\)](#)



Mechanical Performance of Warm-Mixed Porous Asphalt Mixture with Steel Slag and Crumb-Rubber-SBS Modified Bitumen for Seasonal Frozen Regions [\(/1996-1944/12/6/857\)](#)  

Materials **2019**, *12*(6), 857; <https://doi.org/10.3390/ma12060857>

[\(/1996-1944/12/6/857\)](https://doi.org/10.3390/ma12060857) - 14 Mar 2019

Cited by 9 [\(/1996-1944/12/6/857#citedby\)](#) | Viewed by 1528

Open Access Article

  [\(/1996-1944/12/6/856/pdf\)](#)

Biomechanical and Histological Analysis of Titanium (Machined and Treated Surface) Versus Zirconia Implant Materials: An In Vivo Animal Study [\(/1996-1944/12/6/856\)](#)

Materials **2019**, *12*(6), 856; <https://doi.org/10.3390/ma12060856>

[\(/1996-1944/12/6/856\)](https://doi.org/10.3390/ma12060856) - 14 Mar 2019

Cited by 4 [\(/1996-1944/12/6/856#citedby\)](#) | Viewed by 1273

Open Access Article

  [\(/1996-1944/12/6/855/pdf\)](#)

Influence of Process Fluctuations on Residual Stress Evolution in Rotary Swaging of Steel Tubes [\(/1996-1944/12/6/855\)](#)

Materials **2019**, *12*(6), 855; <https://doi.org/10.3390/ma12060855>

[\(/1996-1944/12/6/855\)](https://doi.org/10.3390/ma12060855) - 14 Mar 2019

Cited by 5 [\(/1996-1944/12/6/855#citedby\)](#) | Viewed by 1293

Open Access Article

  [\(/1996-1944/12/6/854/pdf\)](#) 


Mechanical Behaviors of Flax Fiber-Reinforced Composites at Different Strain Rates and Rate-Dependent Constitutive Model [\(/1996-1944/12/6/854\)](#)

Materials **2019**, *12*(6), 854; <https://doi.org/10.3390/ma12060854>

[\(/1996-1944/12/6/854\)](https://doi.org/10.3390/ma12060854) - 13 Mar 2019

Cited by 5 [\(/1996-1944/12/6/854#citedby\)](#) | Viewed by 1171

Open Access Article

  [\(/1996-1944/12/6/853/pdf\)](#) 



Superconducting YBCO Foams as Trapped Field Magnets [\(/1996-1944/12/6/853\)](#)

Materials **2019**, *12*(6), 853; <https://doi.org/10.3390/ma12060853>

[\(/1996-1944/12/6/853\)](https://doi.org/10.3390/ma12060853) - 13 Mar 2019

Cited by 6 [\(/1996-1944/12/6/853#citedby\)](#) | Viewed by 1594

Open Access Communication

  [\(/1996-1944/12/6/852/pdf\)](#)



High-Mobility Inkjet-Printed Indium-Gallium-Zinc-Oxide Thin-Film Transistors Using Sr-Doped Al₂O₃ Gate Dielectric [\(/1996-1944/12/6/852\)](#)

Materials **2019**, *12*(6), 852; <https://doi.org/10.3390/ma12060852>

[\(/1996-1944/12/6/852\)](https://doi.org/10.3390/ma12060852) - 13 Mar 2019

Cited by 6 [\(/1996-1944/12/6/852#citedby\)](#) | Viewed by 1385

Open Access Article

  [\(/1996-1944/12/6/851/pdf\)](#)

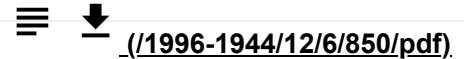
Environmental Assessment of Ultra-High-Performance Concrete Using Carbon, Material, and Water Footprint (/1996-1944/12/6/851)

Materials 2019, 12(6), 851; <https://doi.org/10.3390/ma12060851>

(<https://doi.org/10.3390/ma12060851>) - 13 Mar 2019

Cited by 14 (</1996-1944/12/6/851#citedby>) | Viewed by 2427

Open Access Feature Paper Article



[\(/1996-1944/12/6/850/pdf\)](/1996-1944/12/6/850/pdf)

3D Analysis of Deformation and Porosity of Dry Natural Snow during Compaction (/1996-1944/12/6/850)

Materials 2019, 12(6), 850; <https://doi.org/10.3390/ma12060850>

(<https://doi.org/10.3390/ma12060850>) - 13 Mar 2019

Cited by 1 (</1996-1944/12/6/850#citedby>) | Viewed by 989

Open Access Article



[\(/1996-1944/12/6/849/pdf\)](/1996-1944/12/6/849/pdf)

Cell Viability of Porous Poly(D,L-lactic acid)/Vertically Aligned Carbon Nanotubes/Nanohydroxyapatite Scaffolds for Osteochondral Tissue Engineering (/1996-1944/12/6/849)

Materials 2019, 12(6), 849; <https://doi.org/10.3390/ma12060849>

(<https://doi.org/10.3390/ma12060849>) - 13 Mar 2019

Cited by 5 (</1996-1944/12/6/849#citedby>) | Viewed by 1169

Open Access Article



[\(/1996-1944/12/6/848/pdf\)](/1996-1944/12/6/848/pdf)

Fabrication of Lanthanum Strontium Manganite Ceramics via Agar Gel Casting and Solid State Sintering (/1996-1944/12/6/848)

Materials 2019, 12(6), 848; <https://doi.org/10.3390/ma12060848>

(<https://doi.org/10.3390/ma12060848>) - 13 Mar 2019

Cited by 1 (</1996-1944/12/6/848#citedby>) | Viewed by 1067

Open Access Article



[\(/1996-1944/12/6/847/pdf\)](/1996-1944/12/6/847/pdf)

Functionalisation of Silicone by Drug-Embedded Chitosan Nanoparticles for Potential Applications in Otorhinolaryngology (/1996-1944/12/6/847)

Materials 2019, 12(6), 847; <https://doi.org/10.3390/ma12060847>

(<https://doi.org/10.3390/ma12060847>) - 13 Mar 2019

Cited by 7 (</1996-1944/12/6/847#citedby>) | Viewed by 1207

Open Access Review



[\(/1996-1944/12/6/846/pdf\)](/1996-1944/12/6/846/pdf)

Quality Control of High Carbon Steel for Steel Wires (/1996-1944/12/6/846)

Materials 2019, 12(6), 846; <https://doi.org/10.3390/ma12060846>

(<https://doi.org/10.3390/ma12060846>) - 13 Mar 2019

Cited by 1 (</1996-1944/12/6/846#citedby>) | Viewed by 992

Open Access Article



[\(/1996-1944/12/6/845/pdf\)](/1996-1944/12/6/845/pdf)

Mechanical Performance of Biodegradable Thermoplastic Polymer-Based Biocomposite Boards from Hemp Shivs and Corn Starch for the Building Industry (/1996-1944/12/6/845)

Materials **2019**, 12(6), 845; <https://doi.org/10.3390/ma12060845>

(<https://doi.org/10.3390/ma12060845>) - 13 Mar 2019

Cited by 9 (</1996-1944/12/6/845#citedby>) | Viewed by 895



Open Access Article

[\(/toggle_desktop_layout_cookie\)](#)

[\(/1996-1944/12/6/844/pdf\)](#)

Effects of Alkali Metal (Li, Na, and K) Incorporation in NH₂-MIL125(Ti) on the Performance of CO₂ Adsorption (</1996-1944/12/6/844>)

Materials **2019**, 12(6), 844; <https://doi.org/10.3390/ma12060844>

(<https://doi.org/10.3390/ma12060844>) - 13 Mar 2019

Cited by 5 (</1996-1944/12/6/844#citedby>) | Viewed by 1120



Open Access Article

[\(/1996-1944/12/6/843/pdf\)](#)

Enhanced Electrochemical Performances of Cobalt-Doped Li₂MoO₃ Cathode Materials (</1996-1944/12/6/843>)

Materials **2019**, 12(6), 843; <https://doi.org/10.3390/ma12060843>

(<https://doi.org/10.3390/ma12060843>) - 13 Mar 2019

Cited by 3 (</1996-1944/12/6/843#citedby>) | Viewed by 1018



Open Access Article

[\(/1996-1944/12/6/842/pdf\)](#)

LiFePO₄-Graphene Composites as High-Performance Cathodes for Lithium-Ion Batteries: The Impact of Size and Morphology of Graphene (</1996-1944/12/6/842>)

Materials **2019**, 12(6), 842; <https://doi.org/10.3390/ma12060842>

(<https://doi.org/10.3390/ma12060842>) - 13 Mar 2019

Cited by 6 (</1996-1944/12/6/842#citedby>) | Viewed by 1451



Open Access Article

[\(/1996-1944/12/6/841/pdf\)](#)

Design of Broad Stopband Filters Based on Multilayer Electromagnetically Induced Transparency Metamaterial Structures (</1996-1944/12/6/841>)

Materials **2019**, 12(6), 841; <https://doi.org/10.3390/ma12060841>

(<https://doi.org/10.3390/ma12060841>) - 13 Mar 2019

Cited by 7 (</1996-1944/12/6/841#citedby>) | Viewed by 896

[Show export options](#)

Displaying articles 1-161

[Previous Issue](#)

[Volume 12, March-1 \(/1996-1944/12/5\)](/1996-1944/12/5)

[Next Issue](#)

[Volume 12, April-1 \(/1996-1944/12/7\)](/1996-1944/12/7)

[Materials \(/journal/materials\)](/journal/materials), EISSN 1996-1944, Published by MDPI [Disclaimer](#)

[RSS \(/rss/journal/materials\)](/rss/journal/materials) [Content Alert \(/journal/materials/toc-alert\)](/journal/materials/toc-alert)

[Further Information](#)

[Article Processing Charges \(/apc\)](#)

[Pay an Invoice \(/about/payment\)](#)

[Open Access Policy \(/openaccess\)](#)

[Contact MDPI \(/about/contact\)](#)

[Jobs at MDPI \(https://careers.mdpi.com\)](https://careers.mdpi.com)

 [\(/toggle_desktop_layout_cookie\)](#)  

Guidelines

[For Authors \(/authors\)](#)

[For Reviewers \(/reviewers\)](#)

[For Editors \(/editors\)](#)

[For Librarians \(/librarians\)](#)

[For Publishers \(/publishing_services\)](#)

[For Societies \(/societies\)](#)

MDPI Initiatives

[Institutional Open Access Program \(IOAP\) \(/ioap\)](#)

[Sciforum \(https://sciforum.net\)](https://sciforum.net)

[Preprints \(https://www.preprints.org\)](https://www.preprints.org)

[Scilit \(https://www.scilit.net\)](https://www.scilit.net)

[SciProfiles \(https://sciprofiles.com\)](https://sciprofiles.com)

[MDPI Books \(https://www.mdpi.com/books\)](https://www.mdpi.com/books)

[Encyclopedia \(https://encyclopedia.pub\)](https://encyclopedia.pub)

[JAMS \(https://jams.pub\)](https://jams.pub)

[Proceedings \(/about/proceedings\)](#)

[MDPI Blog \(http://blog.mdpi.com/\)](http://blog.mdpi.com/)


Follow MDPI

[LinkedIn \(https://www.linkedin.com/company/mdpi\)](https://www.linkedin.com/company/mdpi)

[Facebook \(https://www.facebook.com/MDPIOpenAccessPublishing\)](https://www.facebook.com/MDPIOpenAccessPublishing)

[Twitter \(https://twitter.com/MDPIOpenAccess\)](https://twitter.com/MDPIOpenAccess)

Subscribe to receive issue release notifications and newsletters from MDPI journals

Select options 

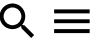
Enter your email address...

MDPI (I)

Subscribe



[\(/toggle_desktop_layout_cookie\)](#)



© 1996-2021 MDPI (Basel, Switzerland) unless otherwise stated

[Disclaimer](#) [Terms and Conditions \(/about/terms-and-conditions\)](#)

[Privacy Policy \(/about/privacy\)](#)



[Sign In / Sign Up \(/user/login\)](#)[Submit \(https://susy.mdpi.com/user/manuscripts/upload?journal=materials\)](https://susy.mdpi.com/user/manuscripts/upload?journal=materials)

Search for Articles:

Advanced Search

[Journals \(/about/journals\)](#) / [Materials \(/journal/materials\)](#) / [Editorial Board](#) /**materials**[\(/journal/materials\)](#)IMPACT
FACTOR
3.057
journal/[Submit to *Materials* \(https://susy.mdpi.com/user/manuscripts/upload?form\[journal_id\]=14\)](https://susy.mdpi.com/user/manuscripts/upload?form[journal_id]=14)[Review for *Materials* \(https://susy.mdpi.com/volunteer/journals/review\)](https://susy.mdpi.com/volunteer/journals/review)

Journal Menu

► Journal Menu

- [Materials Home \(/journal/materials\)](#)
- [Aims & Scope \(/journal/materials/about\)](#)
- [Editorial Board \(/journal/materials/editors\)](#)
- [Reviewer Board \(/journal/materials/submission_reviewers\)](#)
- [Topics Board \(/journal/materials/topic_editors\)](#)
- [Instructions for Authors \(/journal/materials/instructions\)](#)
- [Special Issues \(/journal/materials/special_issues\)](#)
- [Sections & Collections \(/journal/materials/sections\)](#)
- [Article Processing Charge \(/journal/materials/apc\)](#)
- [Indexing & Archiving \(/journal/materials/indexing\)](#)
- [Editor's Choice Articles \(/journal/materials/editors_choice\)](#)
- [Most Cited & Viewed \(/journal/materials/most_cited\)](#)
- [Journal Statistics \(/journal/materials/stats\)](#)
- [Journal History \(/journal/materials/history\)](#)
- [Journal Awards \(/journal/materials/awards\)](#)
- [Society Collaborations \(/journal/materials/societies\)](#)
- [Conferences \(/journal/materials/events\)](#)
- [Editorial Office \(/journal/materials/editorial_office\)](#)

Journal Browser

► Journal Browser

- > [Forthcoming issue \(/1996-1944/14/7\)](#)
- > [Current issue \(/1996-1944/14/6\)](#)

[Vol. 14 \(2021\) \(/1996-1944/14\)](#)

- [Materials Simulation and Design Section \(/journal/materials/sectioneditors/Materials_Simulation_Design\)](#)
- [Electronic Materials Section \(/journal/materials/sectioneditors/electronic_materials\)](#)
- [Advanced and Functional Ceramics Section \(/journal/materials/sectioneditors/Advanced_Functional_Ceramics\)](#)

MDPI

(/toggle_desktop_layout_cookie)



Editors (21)

Prof. Dr. Maryam Tabrizian

[Website \(https://www.mcgill.ca/biomat-x/lab-members/principal-investigator\)](https://www.mcgill.ca/biomat-x/lab-members/principal-investigator) [SciProfiles](#)

Editor-in-Chief

James McGill Professor, Professor of Biomedical Engineering, Professor of Bioengineering, Professor of Experimental Surgery, Department of Biomedical Engineering, Faculty of Medicine/Faculty of Dentistry, Duff Medical Science Building, 3775 University Street, Montreal, QC, H3A 2B4, Canada

Interests: cell-biomaterial interactions; LbL self-assembly systems; theranostic devices for gene/protein therapy and tissue engineering; nanostructured interface by surface molecular engineering; microfluidic platforms for biorecognition systems and Lab-on-a-chip devices; real-time monitoring of cellular activities; characterization of biomaterials debris in biological tissues; polymer synthesis and characterization

[Special Issues and Collections in MDPI journals](#)

Dr. Christof Schneider

[Website \(https://www.psi.ch/en/lmx-interfaces/people/christof-schneider\)](https://www.psi.ch/en/lmx-interfaces/people/christof-schneider)

Associate Editor-in-Chief

Materials Group, General Energy Research Department, Paul Scherrer Institut, CH-5232 Villigen, Switzerland, Lecturer ETH Zurich

Interests: oxide materials for energy applications: thermoelectrics, ion conductors, battery materials; Pulsed Laser Deposition (PLD); multiferroics; interface physics of oxides with strong electronic correlations



Prof. Dr. Filippo Berto

[Website \(https://www.ntnu.edu/employees/filippo.berto\)](https://www.ntnu.edu/employees/filippo.berto) [SciProfiles](#)

Associate Editor-in-Chief

Department of Mechanical and Industrial Engineering, Norwegian University of Science and Technology, 7491 Trondheim, Norway

Interests: fatigue and fracture behavior of materials; mechanical characterization; structural integrity of conventional and innovative materials

[Special Issues and Collections in MDPI journals](#)

Prof. Dr. Guillermo Requena

[Website \(https://www.dlr.de/wf/en/desktopdefault.aspx/tabid-2447/3634_read-5395/\)](https://www.dlr.de/wf/en/desktopdefault.aspx/tabid-2447/3634_read-5395/) [SciProfiles](#)

Associate Editor-in-Chief

Department of Metallic Structures and Hybrid Materials Systems, Institute for Materials Research, German Aerospace Centre, Linder Höhe, 51147, Cologne, Germany

Interests: light alloys; metals for additive manufacturing; three-dimensional material characterization; synchrotron tomography; high energy synchrotron diffraction; aluminum alloys; titanium alloys; magnesium alloys; titanium aluminides; metal matrix composites; phase transformations; relationships microstructure-properties; thermo-mechanical behavior of metals

[Special Issues and Collections in MDPI journals](#)



Dr. Francesco Baino *

[Website \(http://www.composites.polito.it\)](http://www.composites.polito.it) [SciProfiles](#)

Section Editor-in-Chief

Institute of Materials Physics and Engineering, Department of Applied Science and Technology, Politecnico di Torino, Corso Duca degli Abruzzi 24, 10129 Turin, Italy

Interests: bioactive glasses; bioceramics; composites; tissue engineering; multifunctional biomaterials

* Section EIC of Advanced and Functional Ceramics

[Special Issues and Collections in MDPI journals](#)



Dr. Fabrizio Roccaforte *

[Website \(https://www.imm.cnr.it/users/fabrizioroccaforte\)](https://www.imm.cnr.it/users/fabrizioroccaforte) [SciProfiles](#)

Section Editor-in-Chief

CNR-IMM, Strada VIII, n. 5 - Zona Industriale, I-95121 Catania, Italy

Interests: wide band gap semiconductors (WBG); silicon carbide (SiC); gallium nitride (GaN); gallium oxide (Ga₂O₃), metal/semiconductor and metal/oxide/semiconductor interfaces; Schottky diode; JBS; MOSFET; HEMT; WBG device processing; power- and high-frequency electronics

* Section EIC of Electronic Materials

[Special Issues and Collections in MDPI journals](#)



Prof. Dr. Vlassios Likodimos *

Website (http://en.solid.phys.uoa.gr/fileadmin/solid.phys.uoa.gr/upload/htm/Associate_Professors/Likodimos/likodimos_en.html) **SciProfiles**

Section Editor-in-Chief

Section of Condensed Matter Physics, Department of Physics, National and Kapodistrian University of Athens, Panepistimioupoli, 157 84, Athens, Greece

Interests: photocatalytic materials; nanostructured titanium dioxide; carbon nanomaterials; metal oxides

* Section EIC of Materials Physics

Special Issues and Collections in MDPI journals



Prof. Dr. Valery V. Tuchin *

Website (<https://www.sgu.ru/en/person/tuchin-valery-victorovich>) **SciProfiles**

Section Editor-in-Chief

Research-Educational Institute of Optics and Biophotonics, Saratov State University, 410012 Saratov, Russia

Interests: biological and medical physics; biophotonics; biomedical optics; laser spectroscopy and imaging in biomedicine; nonlinear dynamics of laser and optical systems; physics of optical and laser measurements; nanobiophotonics

* Section EIC of Optics and Photonics

Special Issues and Collections in MDPI journals



Prof. Dr. Teofil Jesionowski *

Website (<https://www.fct.put.poznan.pl/pl/kadra/73>) **SciProfiles**

Section Editor-in-Chief

Institute of Chemical Technology and Engineering, Faculty of Chemical Technology, Poznan University of Technology, Berdychowo 4, PL-60965 Poznan, Poland

Interests: biopolymers; synthesis, characterization and applications of advanced functional materials; functional fillers and polymer composites; (bio)additives and eco-friendly fillers; biomineralization-inspired syntheses and extreme biomimetics; biocomposites and biomaterials; removal of wastewater pollutants via adsorption; photocatalysis or precipitation methods; pigment composites; enzyme immobilization; colloid chemistry and surface modification; hybrid systems; biosensors

* Section EIC of Materials Chemistry

Special Issues and Collections in MDPI journals



Prof. Dr. Stefano Bellucci *

Website (http://www.unisrta.com/dipartimenti/fisica-e-scienza-dei-sistemi/prof-stefano-bellucci/?doing_wp_cron=1537925959.0764439105987548828125) **SciProfiles**

Section Editor-in-Chief

INFN-Laboratori Nazionali di Frascati, 00044 Frascati, Italy

Interests: theoretical physics; condensed matter; biophysics; physical chemistry; nanoscience and nanotechnology; nanocarbon-based composites; biomedical applications

* Section EIC of Carbon Materials

Special Issues and Collections in MDPI journals



Prof. Dr. Steven L. Suib *

Website (<https://www.ims.uconn.edu/steven-l-suib/>) **SciProfiles**

Section Editor-in-Chief

Unit 3060, Department of Chemistry, University of Connecticut, 55 N. Eagleville Rd., Storrs, CT 06269-3060, USA

Interests: manganese oxides; catalysis; ceramics; nanotech; microwaves

* Section EIC of Catalytic Materials



Prof. Dr. Seung Hwan Ko *

Website (<http://ants.snu.ac.kr/>) **SciProfiles**

Section Editor-in-Chief

Mechanical Engineering, Seoul National University, Seoul, Korea

Interests: energy devices; wearable electronics; flexible electronics; stretchable electronics; soft robotics; sensors; actuators; electronics

* Section EIC of Smart Materials

Special Issues and Collections in MDPI journals



Prof. Dr. Sanjay Mathur *

Website (<http://www.mathur.uni-koeln.de>) **SciProfiles**

Section Editor-in-Chief

Inorganic and Materials Chemistry, University of Cologne, Institute of Inorganic Chemistry, GreinstraÙe 6, D-50939 Cologne, Germany

Interests: molecular precursor libraries; precursor-derived materials; nanostructured materials; chemical vapor deposition; atomic layer deposition; sol-gel; nanofibers and nanowires; batteries; photovoltaics; solar hydrogen

* Section EIC of Manufacturing Processes and Systems

Special Issues and Collections in MDPI journals



Prof. Dr. Raman Singh *

Website (<https://www.monash.edu/engineering/ramansingh>) **SciProfiles**

Section Editor-in-Chief

Departments of Mechanical & Aerospace Engineering and Chemical Engineering, Monash University, Melbourne Vic 3800, Australia

Interests: materials degradation, corrosion, degradation of polymer and composites

* Section EIC of Corrosion and Materials Degradation

Special Issues and Collections in MDPI journals



Prof. Dr. Rafael Luque *

Website (<https://recognition.webofsciencegroup.com/awards/highly-cited/2020/>) **Website** (<http://www.uco.es/users/q62alsor/>)

Section Editor-in-Chief

Departamento de Química Orgánica, Universidad de Córdoba, Campus de Rabanales, Edificio Marie Curie (C-3), Ctra Nnal IV-A, Km 396, Córdoba, Spain

Interests: green chemistry; biomass valorization; heterogeneous catalysis; nanomaterial design

* Section EIC of Porous Materials

Special Issues and Collections in MDPI journals



Prof. Dr. Pascal Van Der Voort *

Website (<http://www.comoc.ugent.be>) **SciProfiles**

Section Editor-in-Chief

Department of Chemistry, Center for Ordered Materials, Organometallics and Catalysis (COMOC), Faculty of Sciences, Ghent University, Krijgslaan 281 (S3), 9000 Ghent, Belgium

Interests: ordered mesostructures; metal organic frameworks (MOFs); periodic mesoporous organosilicas; Covalent Organic Frameworks; adsorption; catalysis & catalytic materials

* Section EIC of Structure Analysis and Characterization

Special Issues and Collections in MDPI journals



Prof. Dr. Panagiotis G. Asteris *

Website1 (<http://civil.aspete.gr/en/staff-en/panagiotis-asteris>) **Website2** (<https://scholar.google.com/citations?user=DtjDXQUAAAAJ&hl=en>)

SciProfiles

Section Editor-in-Chief

Department of Civil Engineering, School of Pedagogical & Technological Education, Athens, Greece

Interests: sustainability and resilience; reinforced concrete structures; durability

* Section EIC of Materials Simulation and Design

Special Issues and Collections in MDPI journals

Prof. Dr. Eddie Koenders *

Website (<https://www.wib.tu-darmstadt.de/wib/institut.de.jsp>) **SciProfiles**

Section Editor-in-Chief

Institute of Construction and Building Materials, Technical University of Darmstadt, Darmstadt, Germany

Interests: multiscale modeling; modeling hydration and transport; sustainable binders; thermal energy storage; ultralight foams

* Section EIC of Construction and Building Materials

[Special Issues and Collections in MDPI journals](#)



Prof. Dr. Andrei V. Petukhov *

Website (<https://www.uu.nl/staff/APetoukhov/>) **SciProfiles**

Section Editor-in-Chief

1. van 't Hoff laboratory for physical & colloid chemistry, Debye Institute for Nanomaterials Science, Utrecht University, Utrecht, The Netherlands

2. Laboratory of Physical Chemistry, Eindhoven University of Technology, Eindhoven, The Netherlands

Interests: colloids and nanoparticles; self-organisation; colloidal crystals; colloidal liquid crystals; chiral colloids; active matter and dissipative assembly; advanced synchrotron scattering techniques; microscopy at the nanoscale

* Section EIC of Advanced Nanomaterials and Nanotechnology

[Special Issues and Collections in MDPI journals](#)



Prof. Dr. Alessandro Pegoretti *

Website (<http://www.ing.unitn.it/~pegoretti/>) **SciProfiles**

Section Editor-in-Chief

Department of Industrial Engineering, University of Trento, Trento, Italy

Interests: deformation, yield and fracture mechanics of polymers and composites; processing and characterization of multiphase polymeric materials (micro- and nanocomposites, blends); durability of polymeric and composite materials; environmentally sustainable polymers and composites (biodegradable, from renewable resources, fully recyclable); polymers and composites with functional properties (electrical conductivity, shape memory, strain and damage monitoring, self-healing, etc.)

* Section EIC of Advanced Composites

[Special Issues and Collections in MDPI journals](#)



Prof. Dr. Aldo R. Boccaccini *

★ (<https://recognition.webofsciencegroup.com/awards/highly-cited/2020/>) **Website** (<http://www.biomat.techfak.uni-erlangen.org/>)

Section Editor-in-Chief

Institute of Biomaterials, University of Erlangen-Nuremberg, Erlangen, Germany

Interests: biomaterials; bioactive glasses; composites; tissue engineering

* Section EIC of Biomaterials

[Special Issues and Collections in MDPI journals](#)



Previous Editor



Prof. Dr. Andreas Taubert *

Website (<http://www.taubert-lab.net/>) **SciProfiles**

Former Editor-in-Chief

Institute of Chemistry, University of Potsdam, Building 25, Rm. B.0.17-17, Karl-Liebknecht-Str. 24-25, D-14476 Golm, Germany

Interests: inorganic materials synthesis in ionic liquids; functional ionic liquids-hybrid materials; ionogels; biomimetic materials; hybrid materials; calcium phosphate; silica; water treatment; energy materials

* Founding Editor-in-Chief and Former Editor-in-Chief of Materials from 2008 until December 2011.

[Special Issues and Collections in MDPI journals](#)

Editorial Board Members (1082)

Article

Mechanical and Cytocompatibility Evaluation of UHMWPE/PCL/Bioglass[®] Fibrous Composite for Acetabular Labrum Implant

Adhi Anindyajati * , Philip Boughton and Andrew J. Ruys

School of Aerospace, Mechanical and Mechatronic Engineering, University of Sydney, NSW 2006, Australia; philip.boughton@sydney.edu.au (P.B.); andrew.ruys@sydney.edu.au (A.J.R.)

* Correspondence: aani2456@uni.sydney.edu.au

Received: 24 January 2019; Accepted: 8 March 2019; Published: 19 March 2019



Abstract: In this study, a fibrous composite was developed as synthetic graft for labral reconstruction treatment, comprised of ultra-high molecular weight polyethylene (UHMWPE) fabric, ultrafine fibre of polycaprolactone (PCL), and 45S5 Bioglass[®]. This experiment aimed to examine the mechanical performance and cytocompatibility of the composite. Electrospinning and a slurry dipping technique were applied for composite fabrication. To assess the mechanical performance of UHMWPE, tensile cyclic loading test was carried out. Meanwhile, cytocompatibility of the composite on fibroblastic cells was examined through a viability assay, as well as SEM images to observe cell attachment and proliferation. The mechanical test showed that the UHMWPE fabric had a mean displacement of 1.038 mm after 600 cycles, approximately 4.5 times greater resistance compared to that of natural labrum, based on data obtained from literature. A viability assay demonstrated the predominant occupation of live cells on the material surface, suggesting that the composite was able to provide a viable environment for cell growth. Meanwhile, SEM images exhibited cell adhesion and the formation of cell colonies on the material surface. These results indicated that the UHMWPE/PCL/Bioglass[®] composite could be a promising material for labrum implants.

Keywords: UHMWPE/PCL/Bioglass[®]; fibrous composite; labrum implant; cyclic loading; cytocompatibility

1. Introduction

Acetabular labrum is fibrocartilage tissue located in the hip joint, located between the femur and the acetabular rim [1,2]. Biomechanically, it enhances joint stability and seals the joint to protect the fluid inside [1–3]. Tears in this region may hinder hip joint-related activities and in the long term could even progress to osteoarthritis [4–6]. Therefore, it is essential to preserve labrum function. In cases of severe damage, reconstruction is often required, which involves tissue grafting [6–8]. However, there are several limitations associated to autografting, including source availability and the requirement of additional surgical procedures [8,9]. A synthetic graft can be an alternative approach to tackle these drawbacks.

The architecture of acetabular labrum comprises of a fibrous network [10]. To mimic the native tissue, a labrum implant is developed using fibre-based materials. These materials are made into a composite, allowing a combination of different features to be a part of one working system. To withstand mechanical loads working in the labrum area, ultra-high molecular weight polyethylene (UHMWPE) fabric is applied as an implant core or macrostructure. To facilitate cell attachment, growth, and formation of neo tissue, a biodegradable layer of aligned electrospun polycaprolactone (PCL) fibres is applied, covering the fabric. The main structure of acetabular labrum consists of highly oriented

collagen fibril, hence this fine fibres layer can also mimic the natural labrum tissue [10]. Additionally, a bioactive glass coating is added, to further stimulate implant bonding with both bone and soft tissues.

Polyethylene (PE) is widely used as biomaterial. Its biomedical application includes orthopedic and soft tissue reconstruction [11]. Amongst other PE members, UHMWPE is the most widely used and studied, also possesses physical and mechanical properties suitable for load bearing material [11]. Investigation of UHMWPE as fibrocartilage replacement includes application for the meniscus [12], the artificial intervertebral disc [13–17], and the anterior cruciate ligament (ACL) [18]. Used as reinforcement in polyvinyl alcohol (PVA) hydrogel, UHMWPE provides strength to deliver similar tensile stiffness to the meniscus in a circumferential direction [12]. UHMWPE fibres were also composited with PVA cords to develop ACL replacement [18]. This composite showed tensile behaviour within the range of the native ligament and showed endurance in fatigue testing simulating normal activities.

More extensive research on UHMWPE was conducted to develop an artificial intervertebral disc (AID) [13–17]. UHMWPE woven filaments were coated with low-density polyethylene (LDPE) and sprayed with bioactive ceramic in their upper and lower surfaces. A torsional test showed comparable value to a human intervertebral disc [13]. Fatigue testing in saline solution demonstrated the implant durability, without strength deterioration and debris [15]. Simulation of dynamic body motion on UHMWPE fabric demonstrated a hysteresis loss curve similar to that of natural tissue and potential durability of more than 30 years [16]. Subsequent tests using a simulated vertebral body confirmed the physical endurance of the UHMWPE-based implant [17]. A creep test also demonstrated implant flexibility similar to that of a normal disc [10]. Furthermore, UHMWPE fabric has been applied in clinical settings [19,20] and the literature reported on the fatigue and abrasion resistance of this material as an intervertebral disc and ACL replacement [7,9–11]. It could be a promising material for acetabular labrum implants and therefore its mechanical performance for this particular application requires investigation.

Polycaprolactone (PCL) is a biodegradable and biocompatible polymer, which has acquired approval from the Food and Drug Administration (FDA) as a medical device [21,22]. This material has been broadly studied as a scaffold for fibrocartilage tissue engineering, and has already reached the preclinical stage [23,24]. Applications on fibrocartilage scaffolds included those for the meniscus [25–27], vertebral discs [28], cartilage [29,30], and musculoskeletal tissue [31]. The performance of electrospun PCL was also examined in cell culture [25,26,28,29,31–34]. These studies reported favourable results, where fibrous PCL was able to support cell growth. The electrospun PCL layer facilitated chondrocytes to adhere, spread, and produce an extracellular matrix (ECM) [34]. Fibre alignment was directive to cells orientation, morphology, attachment, distribution, and production of extracellular matrix production [26,31,32]. Another study on intervertebral disc tissue engineering reported that bovine mesenchymal stem cells (MSCs) seeded on electrospun PCL could mimic the native cells and formed ECM similar to annulus fibrosus, the fibrous part of the intervertebral disc [28]. Based on these reports, electrospun PCL could also be a promising material for labrum implants, specifically to attract cell attachment and provide a temporary environment, or scaffold, for cell growth and neo-tissue formation.

Bioglass[®] is a highly bioactive material and has been used clinically in hard tissue reconstruction [35–37]. It has also exhibited potential in facilitating soft tissue bonding [9,38,39]. On soft tissue engineering applications, bioactive glass demonstrated promising outcomes, including in implant-soft tissue integration, vascularization, control of degradation rate, and promoting chondrogenesis [37,40–47]. In fibrocartilage replacement, bioactive glass was applied as a coating and was reported to be capable of stimulating bonding between implant and bone tissue [15,43,48]. Development of the acetabular labrum implant could exploit the potential benefits of bioactive glass. The use of bioactive glass coating is expected to promote implant integration with surrounding tissue, improve implant stabilization, and even enhance the healing progress. Ability to integrate to surrounding tissue determines implant performance, mainly in stability [16,43,49,50].

Bioactive material could improve implant stabilization through facilitating biological bonding with surrounding bone tissue [15,36,51]. Therefore, the potential capability of bioactive glass to bond with both hard and soft tissues could be beneficial for labrum implants, since the labrum was connected to both tissues.

A labrum implant is proposed as an alternative approach to enhance labral repair and healing. Extensive studies have been conducted on fibrocartilage implants, such as in the meniscus, the anterior cruciate ligament, intervertebral discs and the temporomandibular joint. However, investigation on the labrum implant is still limited. In this study, an implant to assist labral reconstruction was developed using a novel approach, which was fibrous composite containing UHMWPE fabric, electrospun PCL and bioactive glass. Electrospinning was applied to form a fibrous PCL layer on UHMWPE fabric, followed by slurry dipping to introduce Bioglass[®] coating [52]. These methods were relatively simple, yet effective for producing the UHMWPE/PCL/Bioglass[®] composite.

The purpose of this study was to investigate the UHMWPE/PCL/Bioglass[®] composite for acetabular labrum implants through mechanical testing and *in vitro* observation. To evaluate the mechanical performance of UHMWPE fabric as a load bearing structure, a cyclic loading test was carried out and the output was compared to the results of similar test on acetabular labrum reported in the literature [53]. This test was conducted as labrum tissue was not exposed to singular, high tensile load, but to repetitive loading at relatively lower forces [53]. Besides, the available data on the labrum provided by this test could be used for comparison.

To assess the biocompatibility of the composite, an *in vitro* test was conducted to examine cell responses towards the material surface, including attachment, adhesion, and spreading. These behaviours influence implant—tissue integration, which sequentially defines successful implantation [54]. A biocompatibility test on *in vitro* cell culture could also predict the performance of biomedical material on biological environments. Similar effects of 45S5 Bioglass[®] on osteoblasts, fibroblasts, and macrophages were detected on both *in vitro* and *in vivo* experiments [55]. Bioactive glass could support fibroblast viability and proliferation [56–62], but some studies found that it also had an inhibitive effect on proliferation depending on the amount [63,64]. In this study, fibroblast response on UHMWPE/PCL/Bioglass[®] composite was investigated, along with their behaviour on UHMWPE fabric and UHMWPE/PCL composite. Assessment on UHMWPE/PCL was to observe if the ultrafine PCL fibres could improve cell attachment. Meanwhile, the effect of Bioglass[®] on cell viability was examined by culturing the cells in the UHMWPE/PCL/Bioglass[®] composite. Cell behaviour on UHMWPE fabric is also limitedly reported, unlike those on flat and solid surfaces [65–69]. Therefore, this study is also expected to gain further insights on the cytocompatibility of polyethylene fabric.

2. Materials and Methods

2.1. Electrospinning

Polycaprolactone pellets (Mw 80.000) were dissolved in acetone (Barnes, Sydney, Australia) overnight to make an electrospinning solution with 10% w/v concentration. The electrospinning collector was a rotating aluminium mandrel featuring covered gaps [70]. Parameter setting for the process was flow rate, working distance, and mandrel rotation of 4.5 mL/h, of 12.5 cm, and 1500 RPM, respectively. PCL solution was dispensed from a 10 mL syringe with a 20 G needle onto the grounded collector. A van der Graaf generator (Serrata, Dural, Australia) was connected to the needle tip to generate an electrical charge into the polymer solution. A syringe pump (Injectomat Tiva Agilia, Fresenius Kabi AG, Bad Homburg, Germany) was used to adjust the flow rate.

2.2. Fabrication of UHMWPE/PCL

Two steps of electrospinning were carried out, as depicted in Figure 1. The first step was to form the layer of aligned PCL fibres in the bottom side. After the PCL fibres deposited on the collector, UHMWPE fabric (DSM Dyneema SK78, Dimension-Polyant, Kempen, Germany) patches were then

placed onto it, in the gap area of the collector. PCL/acetone solution was then applied at the edges of these patches, acting as glue to attach the fabric to the fibres. The second step was then initiated after the PCL glue dried, to form a layer of PCL fibres covering the upper side. The result was UHMWPE fabric patches laminated with electrospun fibre, termed PE/PCL.

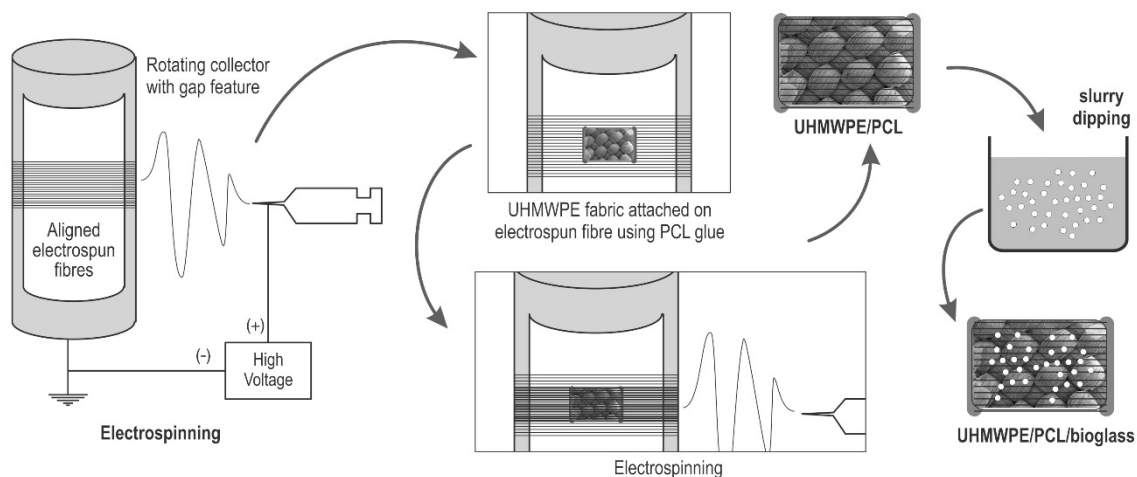


Figure 1. Fabrication process of ultra-high molecular weight polyethylene (UHMWPE)/polycaprolactone (PCL)/Bioglass[®].

2.3. Bioglass[®] Coating

The obtained PE/PCL samples were then coated with Bioglass[®] particles using a slurry dipping method (Figure 1) [71,72]. The 45S5 Bioglass[®] was sourced from the earlier study conducted in our research group. The melt-derived glass particles (<100 μm) were then suspended in demineralised water to make a slurry with 5% w/v concentration, followed by 30 min stirring using a magnetic stirrer. Coating was later applied by gently immersing the PE/PCL patch using tweezers to the slurry for 5 min. The PE/PCL/Bioglass[®] samples (termed as PE/PCL/BG) were then dried in room temperature.

2.4. Cyclic Loading Test of UHMWPE Fabric

Samples of UHMWPE fabric were divided into two groups (5 samples each): not folded (10 mm \times 70 mm) and folded (20 mm \times 70 mm folded into 10 mm \times 70 mm size). The testing method followed the procedure of a cyclic displacement test on acetabular labrum and tissue grafts for hip labral reconstruction [53]. This test was performed using an Instron 8501 Digital and Computerised Fatigue Testing Machine (Norwood, MA, USA). The sample was clamped at 2 cm from each end and the distance between clamps was set at 3 cm. Custom aluminium clips and sandpaper were used to hold the sample and prevent slippage. Sample width and length were measured using a digital calliper. Tensile preload was set at 20 N and sinusoidal cyclic loading was then applied from 20 to 50 N for 100 cycles at 0.5 Hz. Maximum load was increased by 50 N after every 100 cycles, until failure or completion of 100 cycles at 300 N. Cyclic displacement was recorded after 100, 200, 300, 400, 500, and 600 cycles.

2.5. Cell Culture and Seeding

Mouse skin fibroblast (3T3-L1) cells were cultured in Dulbecco's Modified Eagle Medium (DMEM) supplemented with 2.5% antibiotic, 1.25% glutamax, and 1.25% fetal bovine serum (FBS) for 7 days before seeding. Cells responses were assessed using samples of UHMWPE fabric (PE), UHMWPE/PCL (PE/PCL) and UHMWPE/PCL/Bioglass[®] (PE/PCL/BG). The samples were placed in 24-well culture plates and sterilised prior to seeding by immersion in 70% ethanol for 6 h. The samples were rinsed three times in phosphate buffered saline (PBS), followed by 24 h incubation in DMEM to enhance cell attachment [73]. Cell seeding was carried out using the static surface seeding method, then the

samples were incubated for 3 h to facilitate initial cell attachment and immersed in supplemented DMEM to support cell growth [74]. The culture medium was replaced every two days.

2.6. Viability Assay

Cell viability on composite surfaces (PE/PCL and PE/PCL/BG) was assessed after one and seven days of culture. Prior to imaging, the cells-seeded samples were prepared by rinsing in PBS, then incubation in fluorescence solution (1 μ L calcein-AM, 1 μ L propidium iodide, and 1 mL PBS; Sigma Aldrich, Castle Hill, NSW, Australia). Calcein-AM and propidium iodide (PI) were used as marker for live and dead cells, respectively. Fluorescence imaging was carried out using an Olympus BX51 microscope (Olympus Corporation, Tokyo, Japan). Images obtained from the microscope were processed using Fiji ImageJ software (National Institutes of Health, Bethesda, MD, USA).

2.7. Scanning Electron Microscopy

Scanning electron microscope (SEM) imaging was performed to observe cell morphology and attachment on composite surfaces after one, three, and seven days of culture. Samples without cells were also imaged to examine the effect of culture medium and the presence of cells on the materials morphology. Samples were prepared by fixation in 2.5% glutaraldehyde, dehydration in a graded series of ethanol concentrations (30%, 50%, 70%, 90%, 95%, and 100%) and hexamethyldisilazane (HMDS), and gold coated using sputter method. Imaging was carried out using Zeiss Ultra Plus (Carl Zeiss AG, Oberkochen, Germany).

3. Results

Cyclic Loading Test of UHMWPE Fabric

Results from a cyclic loading test on UHMWPE fabric samples were presented in Table 1 and Figure 2, along with the data of acetabular labrum [53]. The fabric exhibited a far lower mean elongation than that of acetabular labrum. After 600 cycles, the unfolded fabric had a mean displacement of 1.038 mm, while the labrum showed 4.53 mm. At this point, displacement resistance of the single layer UHMWPE fabric (unfolded samples) was approximately 4.5 times greater than the native labrum, and the double layer fabric (folded samples) demonstrated even greater resistance, approximately 10 times.

Fibroblast cells residing on PE/PCL and PE/PCL/BG composites were imaged using fluorescence microscopy, as depicted in Figure 3. These images showed live cells (green) and dead cells (red) after one and seven days of culture. Both composites were predominantly occupied by live cells, suggesting that these materials were able to provide a viable environment. At day one, fewer cells were observed on the PE/PCL/BG sample compared to the PE/PCL. Nevertheless, both groups exhibited a comparable cell occupation area and proportion of live cells after seven days of culture. Fibrous PCL was known as a favourable material capable of supporting fibroblasts growth [25,26,28,29,31–34]. On the other hand, the cytocompatibility of bioactive glass is dose-dependent [63,64]. Hence, this finding suggested that the amount of Bioglass[®] in the composite was suitable, as it did not induce an adverse effect on fibroblast growth.

Table 1. Displacement of UHMWPE fabric and human acetabular labrum from the cyclic loading test.

Cycle (Load)	Mean Displacement (mm)		
	Labrum [53]	UHMWPE Fabric	Folded UHMWPE Fabric
0–100 (20–50 N)	0.68	0.153	0.106
0–200 (20–100 N)	1.53	0.331	0.200
0–300 (20–150 N)	2.28	0.486	0.269
0–400 (20–200N)	2.99	0.625	0.326
0–500 (20–250 N)	3.75	0.806	0.378
0–600 (20–300 N)	4.53	1.038	0.426

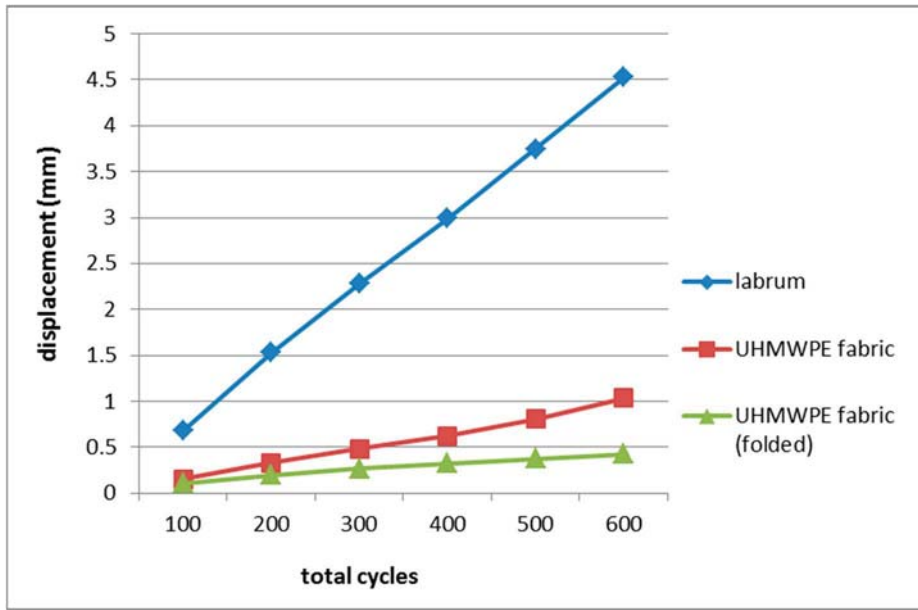
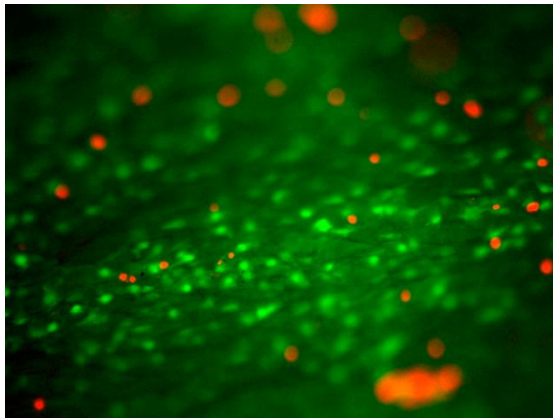
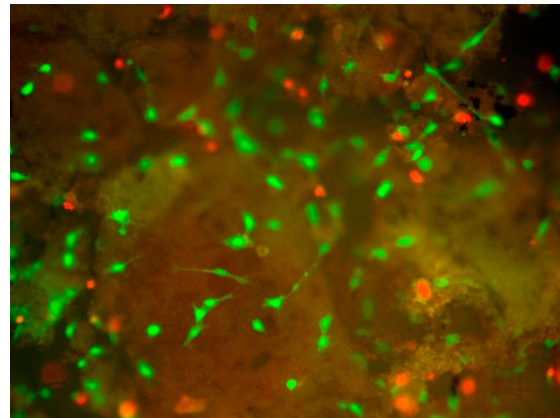


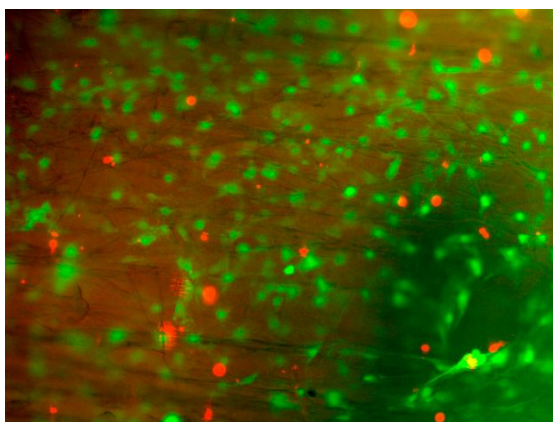
Figure 2. Displacement vs cycles of human acetabular labrum [53] and UHMWPE fabric. Both groups of fabric demonstrated higher resistance to deformation than human acetabular labrum.



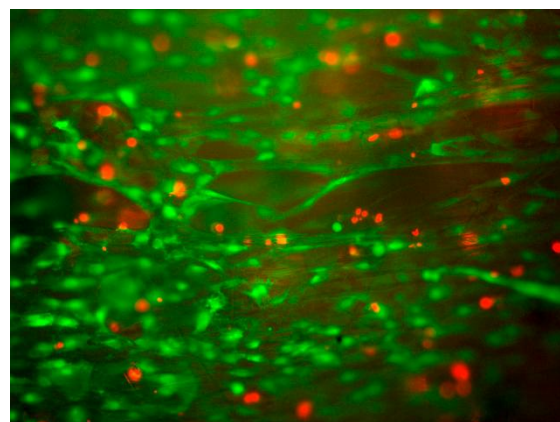
(a) PE/PCL, day 1



(b) PE/PCL/BG, day 1



(c) PE/PCL, day 7



(d) PE/PCL/BG, day 7

Figure 3. Live (green) and dead (red) cells on PE/PCL (a,c) and PE/PCL/BG composites (b,d) after one (a,b) and seven (c,d) days of culture.

Cell morphology and attachment on PE, PE/PCL, and PE/PCL/BG samples after one, three, and seven days of culture are presented in Figures 4–6. On day one, flat cells were observed on the UHMWPE fabric (Figure 4a,d). These cells tended to take place between fabric threads. Cells attached on PE/PCL were spread and elongated to the surrounding fibres, and also appeared bigger than those on the UHMWPE fabric (Figure 4b,e). Meanwhile, fibroblasts exhibited mixed morphology on the PE/PCL/BG sample. Some cells were spread and elongated similar to those on the PE/PCL surface (Figure 4c), while the others showed spread and a more rounded structure (Figure 4f). Cells on PE/PCL and PE/PCL/BG exhibited similar morphology and took place between fibres by holding on the surrounding fibres.

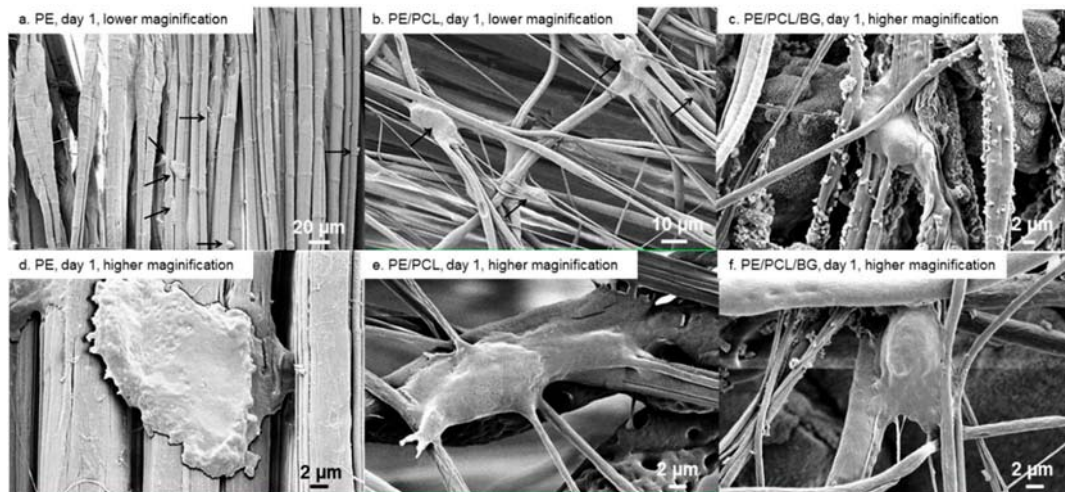


Figure 4. Fibroblast attachment on PE fabric (a,d), PE/PCL (b,e), and PE/PCL/BG (c,f) on day one at lower (a,b) and higher (c–f) magnification. Arrows show cells.

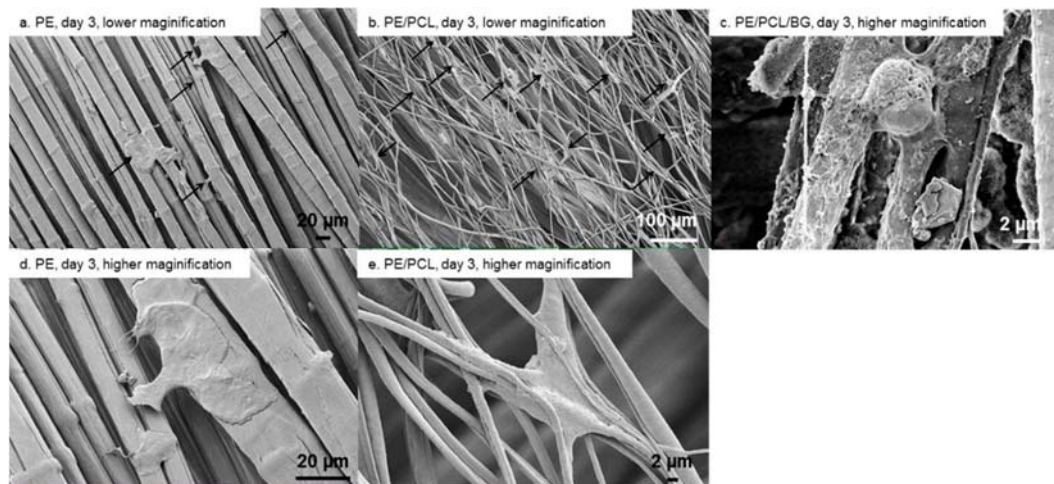


Figure 5. Fibroblast attachment on PE fabric (a,d), PE/PCL (b,e), and PE/PCL/BG (c) on day three at lower (a,b) and higher (c–e) magnification. Arrows show cells.

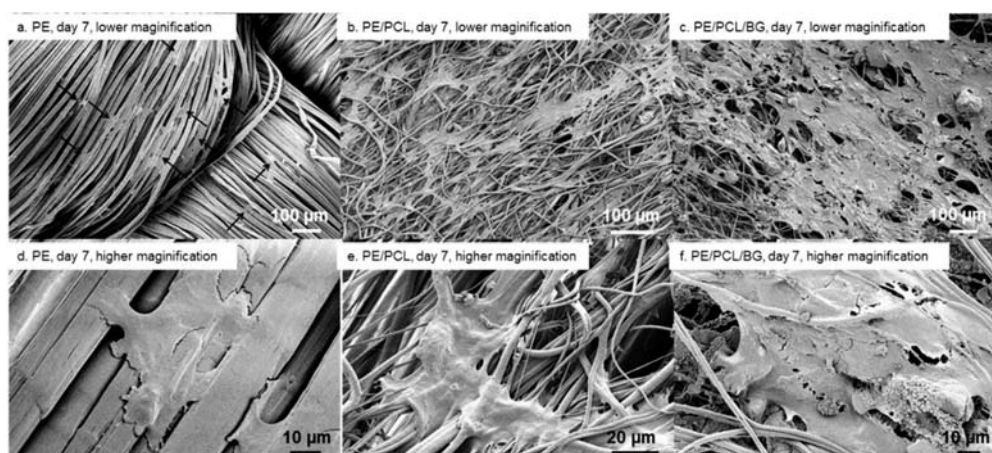


Figure 6. Fibroblast attachment on PE fabric (a,d), PE/PCL (b,e), and PE/PCL/BG (c,f) on day seven at lower (a–c) and higher (d–f) magnification. Arrows show cells.

After incubation for three days, cells on the UHMWPE fabric showed spreading and elongation to the adjacent fibres (Figure 5a,d), although they spread less when compared to those on the PCL fibres layer. These cells were flat in shape and took place between fabric threads. This behaviour was similar to cell response toward PCL fibres after 24 h of culture. At this time point, the PE/PCL composite showed cell colonization on the PCL fibres layer, although the cell form was not different than that on day one (Figure 5b,e). Cells on the PE/PCL/BG sample were difficult to recognize due to their identical appearance to Bioglass[®] particles, although generally the cells were flat shaped with attachment sites on the nearby fibres (Figure 5c).

After 7 days of culture, cells residing on the UHMWPE fabric showed flat and broad morphology, bridging between adjacent fibres (Figure 6a,d). Small cell colonies were also formed. On the PE/PCL sample, cell colonies spread wider, covering a larger area of the PCL fibres layer (Figure 6b). These cells spread following fibre direction and formed an even bigger colony than those at previous time points. These cells also showed more attachment sites anchoring at the neighbouring fibres (Figure 6e). Meanwhile, cells on PE/PCL/BG also spread following fibre direction and formed a larger colony covering the composite surface, attaching on PCL fibres and among Bioglass[®] particulates (Figure 6c,f). Cells on both PE/PCL and PE/PCL/BG also appeared to be more stretched and broader in shape compared to those on the UHMWPE fabric.

Cell proliferation and morphological changes were a function of the culture period, as indicated in Figures 4–6. Cells on all material groups showed broader shape on day three, with more apparent spreading and elongation after seven days of culture. On PE/PCL samples, cell colonies started to form on day three, while cell proliferation on other groups was apparent on day seven. On the longest culture period, the PE/PCL and PE/PCL/BG composites exhibited noticeably larger cell occupation than the pure UHMWPE fabric.

The morphology of the UHMWPE fabric, PCL fibres, and Bioglass[®] particles after immersion in culture medium without the presence of cells are presented in Figure 7. Based on Figures 4–7, there was no noticeable alteration on the UHMWPE fabric and PCL fibres in respect of the culture period and the presence of cells, suggesting the stability of these materials in culture media and cellular environments. Seven days of culture might have no noticeable effect, as UHMWPE is biologically inert [75] and PCL is a slowly degradable material [21]. Meanwhile, rough surface and nanospheres formation were observed in the bioactive glass particles (Figure 7c,f,i), which was likely a formation of an amorphous apatite layer [76,77]. This formation might contain calcite and the amorphous phase of calcium phosphate, which could grow on the superficial layer of 45S5 Bioglass[®] particles when exposed to a culture medium, such as DMEM [78]. These dissolution products could be

potentially beneficial, in terms of promoting bonding to surrounding tissues [9] and angiogenic effects for neovascularization [58,79].

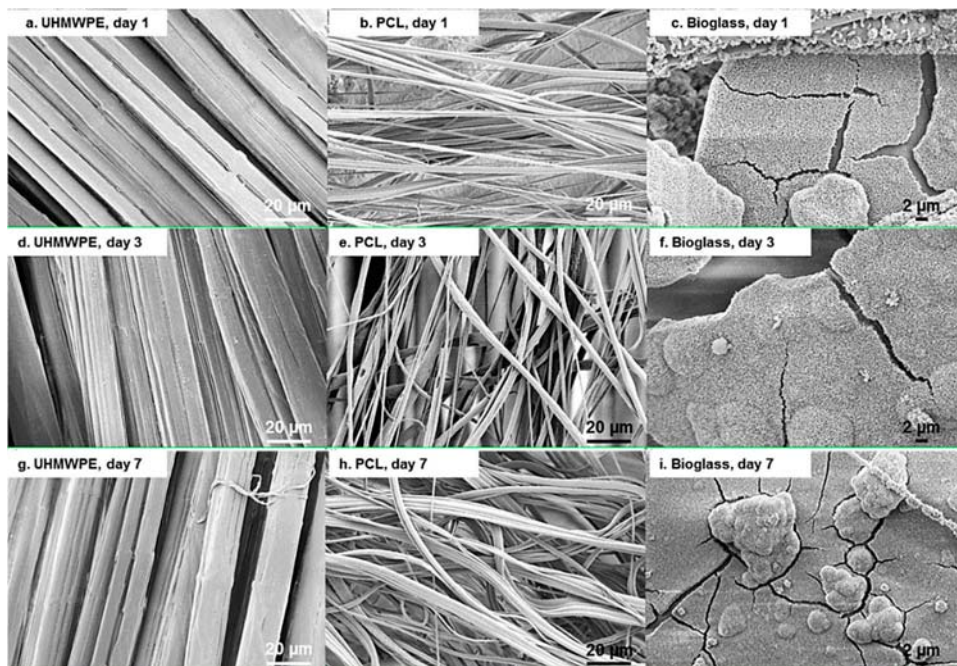


Figure 7. SEM images of UHMWPE fabric (a,d,g), PCL fibres (b,e,h), and Bioglass® particles (c,f,i) after immersion in cell culture medium without cells.

4. Discussion

The UHMWPE fabric exhibited far greater resistance to deformation compared to the native labrum, demonstrating its potential capability to perform as suction seal in the hip joint, a function carried by acetabular labrum. After reconstruction, a graft construct might endure excessive stretching, which might affect the sealing function [53]. A more robust material, such as the UHMWPE fabric tested in this study, could potentially provide a tougher seal. The fabric would also be mechanically superior to tissue grafts in sustaining cyclic loading, as labrum and tissue grafts for labral reconstruction showed comparable cyclic loading behaviour [53]. This test simulated activities from a rehabilitation period post-surgery, thus the greater deformation resistance demonstrated by the fabric also suggested potential durability for long term use. A hip joint could experience around 2 million loading cycles per year, or 5000 cycles per day from walking activity [53,80]. This cyclic loading test has showed that UHMWPE fabric had the potential strength and durability for labrum implants. Follow-up investigations could then involve tests with more loading cycles to assess the mechanical performance of UHMWPE fabric as a labrum implant in normal activity.

Cell morphology can be an indicator to evaluate if a substrate is capable of supporting adhesion. Poor adhesion is signified by rounded and less spread morphology, while flat, broadened and elongated shape indicate good adhesion [54,66,81]. Cells adhered on the UHMWPE fabric were flat-shaped (Figure 6d), demonstrating a positive response toward pure fabric. On the layer of PCL fibres, fibroblasts were more spread out and flattened (Figure 6c,f), indicating that the presence of the electrospun fibres further enhanced cellular attachment. Cell morphology also influences proliferation, in which flattened, and well spread cells, split faster than those in a rounded shape [77]. This also explains the higher proliferation on PCL fibres compared to UHMWPE fabric surface.

Fluorescence and SEM images suggested that Bioglass® could provide viable environment for fibroblasts, as also reported in several studies [61,62]. Fibroblasts could attach on Bioglass® surface and showed elongated shape in long term culture, suggesting a favourable surface for attachment [59,62].

However, cell occupation on PE/PCL/BG sample was lower than that on the PE/PCL sample, particularly in the earlier culture period. It was possibly due to higher pH and Ca ions leaching on Bioglass[®]-contained samples [61,63,82]. Nevertheless, this inhibitive effect was not related to toxicity [82]. On day seven, cells appeared to form a colony covering the surface of the PE/PCL/BG (Figures 3d and 6c), demonstrating that Bioglass[®] could support cell proliferation in the longer term. The presence of Bioglass[®] appeared to halt cell growth in a short time period, but increased growth was observed in longer time periods [59]. Results from fluorescence and SEM images were in agreement, indicating that the amount of Bioglass[®] in the composite was not prohibitive on fibroblasts growth.

Addition of Bioglass[®] in the labrum implant aimed to stimulate bonding between the implant and the host tissue. Bioactive substances, including Bioglass[®], could promote biological bonding [15,36,51], as well as enhance implant stability [16,43,49,50]. As the amount of bioactive glass could affect fibroblast growth [63,64], identification of the appropriate amount is essential. Cytocompatibility test in this study showed the favourable effect of Bioglass[®] on cells growth, indicating suitable Bioglass[®] content in the composite. This result further demonstrated the potential biological compatibility of this composite in vivo, since cell response to Bioglass[®] was reported to be similar in both in vitro and in vivo settings [55]. Further studies could address the mechanical performance and biocompatibility of this composite in an animal model, including the efficacy of Bioglass[®] in promoting implant bonding to the surrounding tissues.

5. Conclusions

Mechanical testing and cytocompatibility analysis in this study demonstrated that the UHMWPE/PCL/Bioglass[®] composite could be a promising material for labrum implants. Tensile cyclic loading testing showed that UHMWPE fabric had greater resistance to displacement, approximately 4.5 times higher than labrum tissue and tissue grafts for labral replacement. This suggested that the fabric had the potential capability to function as a suction seal on the hip joint, as well as showing a promising durability as an artificial graft for labrum replacements. Observations on fibroblasts attachment, morphology, and viability suggested that the UHMWPE/PCL/Bioglass[®] composite was cytocompatible. The presence of electrospun PCL fibres layers enhanced cell attachment, morphology, and proliferation. The addition of Bioglass[®] particles also supported cell growth, suggesting that the added amount was appropriate and effective. These results laid the groundwork for further in vivo investigations examining mechanical performance and biocompatibility of UHMWPE/PCL/Bioglass[®] composite. Further tests could also address implant design, prototyping, and surgical procedure.

Author Contributions: Conceptualization, A.A. and P.B.; Methodology, A.A.; Validation, A.A., P.B. and A.J.R.; Formal Analysis, A.A.; Investigation, A.A.; Resources, P.B. and A.J.R.; Data Curation, A.A.; Writing-Original Draft Preparation, A.A.; Writing-Review & Editing, A.A., P.B. and A.J.R.; Visualization, A.A.; Supervision, P.B. and A.J.R.; Project Administration, A.A.; Funding Acquisition, A.J.R.

Funding: This study was undertaken as a part of PhD program funded by Australia Awards.

Acknowledgments: The authors acknowledge the facilities and the scientific and technical assistance of the Australian Microscopy and Microanalysis Research Facility at the Australian Centre for Microscopy and Microanalysis at the University of Sydney.

Conflicts of Interest: The authors declare no conflict of interest. The founding sponsors had no role in the design of the study; in the collection, analyses, or interpretation of data; in the writing of the manuscript, and in the decision to publish the results.

References

1. Seldes, R.M.; Tan, V.; Hunt, J.; Katz, M.; Winiarsky, R.; Robert, H.; Fitzgerald, J. Anatomy, histologic features, and vascularity of the adult acetabular labrum. *Clin. Orthop. Relat. Res.* **2001**, *382*, 232–240. [[CrossRef](#)]
2. Grant, A.D.; Sala, D.A.; Davidovitch, R.I. The labrum: Structure, function, and injury with femoro-acetabular impingement. *J. Child. Orthop.* **2012**, *6*, 357–372. [[CrossRef](#)] [[PubMed](#)]

3. Ferguson, S.J.; Bryant, J.T.; Ganz, R.; Ito, K. The acetabular labrum seal: A poroelastic finite element model. *Clin. Biomech.* **2000**, *15*, 463–468. [[CrossRef](#)]
4. Ganz, R.; Parvizi, J.; Beck, M.; Leunig, M.; Notzli, H.; Siebenrock, K.A. Femoroacetabular impingement: A cause for osteoarthritis of the hip. *Clin. Orthop. Relat. Res.* **2003**, *417*, 112–120.
5. McCarthy, J.C.; Noble, P.C.; Schuck, M.R.; Wright, J.; Lee, J. The otto e. Aufranc award: The role of labral lesions to development of early degenerative hip disease. *Clin. Orthop. Relat. Res.* **2001**, *393*, 25–37. [[CrossRef](#)]
6. Ejnisman, L.; Philippon, M.J.; Lertwanich, P. Acetabular labral tears: Diagnosis, repair, and a method for labral reconstruction. *Clin. Sports Med.* **2011**, *30*, 317–329. [[CrossRef](#)]
7. Sierra, R.; Trousdale, R. Labral reconstruction using the ligamentum teres capitis: Report of a new technique. *Clin. Orthop. Relat. Res.* **2009**, *467*, 753–759. [[CrossRef](#)]
8. Matsuda, D.K. Arthroscopic labral reconstruction with gracilis autograft. *Arthrosc. Tech.* **2012**, *1*, e15–e21. [[CrossRef](#)]
9. Hench, L.L. Biomaterials: A forecast for the future. *Biomaterials* **1998**, *19*, 1419–1423. [[CrossRef](#)]
10. Petersen, W.; Petersen, F.; Tillmann, B. Structure and vascularization of the acetabular labrum with regard to the pathogenesis and healing of labral lesions. *Arch. Orthop. Trauma Surg.* **2003**, *123*, 283–288. [[CrossRef](#)]
11. Pruitt, L.A.; Chakravartula, A.M. *Mechanics of Biomaterials: Fundamental Principles of Implant Design*; Cambridge University Press: Cambridge, UK, 2011.
12. Holloway, J.L.; Lowman, A.M.; Palmese, G.R. Mechanical evaluation of poly(vinyl alcohol)-based fibrous composites as biomaterials for meniscal tissue replacement. *Acta Biomaterialia* **2010**, *6*, 4716–4724. [[CrossRef](#)] [[PubMed](#)]
13. Kadoya, K.; Kotani, Y.; Abumi, K.; Takada, T.; Shimamoto, N.; Shikinami, Y.; Kadosawa, T.; Kaneda, K. Biomechanical and morphologic evaluation of a three-dimensional fabric sheep artificial intervertebral disc in vitro and in vivo analysis. *Spine* **2001**, *26*, 1562–1569. [[CrossRef](#)]
14. Kotani, Y.; Abumi, K.; Shikinami, Y.; Takada, T.; Kadoya, K.; Shimamoto, N.; Ito, M.; Kadosawa, T.; Fujinaga, T.; Kaneda, K. Artificial intervertebral disc replacement using bioactive three-dimensional fabric: Design, development, and preliminary animal study. *Spine* **2002**, *27*, 929–936. [[CrossRef](#)] [[PubMed](#)]
15. Takahata, M.; Kotani, Y.; Abumi, K.; Shikinami, Y.; Kadosawa, T.; Kaneda, K.; Minami, A. Bone ingrowth fixation of artificial intervertebral disc consisting of bioceramic-coated three-dimensional fabric. *Spine* **2003**, *28*, 637–644. [[CrossRef](#)] [[PubMed](#)]
16. Shikinami, Y.; Kotani, Y.; Cunningham, B.W.; Abumi, K.; Kaneda, K. A biomimetic artificial disc with improved mechanical properties compared to biological intervertebral discs. *Adv. Funct. Mater.* **2004**, *14*, 1039–1046. [[CrossRef](#)]
17. Shikinami, Y.; Kawabe, Y.; Yasukawa, K.; Tsuta, K.; Kotani, Y.; Abumi, K. A biomimetic artificial intervertebral disc system composed of a cubic three-dimensional fabric. *Spine J.* **2010**, *10*, 141–152. [[CrossRef](#)]
18. Bach, J.S.; Detrez, F.; Cherkaoui, M.; Cantournet, S.; Ku, D.N.; Corté, L. Hydrogel fibers for ACL prosthesis: Design and mechanical evaluation of PVA and PVA/UHMWPE fiber constructs. *J. Biomech.* **2013**, *46*, 1463–1470. [[CrossRef](#)]
19. Guidoin, M.-F.; Marois, Y.; Bejui, J.; Poddevin, N.; King, M.W.; Guidoin, R. Analysis of retrieved polymer fiber based replacements for the acl. *Biomaterials* **2000**, *21*, 2461–2474. [[CrossRef](#)]
20. Karaman, A.I.; Kir, N.; Belli, S. Four applications of reinforced polyethylene fiber material in orthodontic practice. *Am. J. Orthod. Dentofacial Orthop.* **2002**, *121*, 650–654. [[CrossRef](#)]
21. Hutmacher, D.W. Scaffolds in tissue engineering bone and cartilage. *Biomaterials* **2000**, *21*, 2529–2543. [[CrossRef](#)]
22. Li, W.-J.; Cooper, J.A., Jr.; Mauck, R.L.; Tuan, R.S. Fabrication and characterization of six electrospun poly(α -hydroxy ester)-based fibrous scaffolds for tissue engineering applications. *Acta Biomaterialia* **2006**, *2*, 377–385. [[CrossRef](#)] [[PubMed](#)]
23. Elliott, D.M.; Mauck, R.L.; Shah, R.P.; Schaer, T.P.; Maher, S.A. 5.524—Biomaterials for replacement and repair of the meniscus and annulus fibrosus. In *Comprehensive Biomaterials*; Ducheyne, P., Ed.; Elsevier: Oxford, UK, 2011; pp. 317–332.
24. Gantenbein-Ritter, B.; Sakai, D. 6.612—Biomaterials for intervertebral disc regeneration. In *Comprehensive Biomaterials*; Ducheyne, P., Ed.; Elsevier: Oxford, UK, 2011; pp. 161–169.

25. Baker, B.M.; Gee, A.O.; Metter, R.B.; Nathan, A.S.; Marklein, R.A.; Burdick, J.A.; Mauck, R.L. The potential to improve cell infiltration in composite fiber-aligned electrospun scaffolds by the selective removal of sacrificial fibers. *Biomaterials* **2008**, *29*, 2348–2358. [[CrossRef](#)] [[PubMed](#)]
26. Baker, B.M.; Mauck, R.L. The effect of nanofiber alignment on the maturation of engineered meniscus constructs. *Biomaterials* **2007**, *28*, 1967–1977. [[CrossRef](#)] [[PubMed](#)]
27. Fisher, M.B.; Henning, E.A.; Söegaard, N.; Esterhai, J.L.; Mauck, R.L. Organized nanofibrous scaffolds that mimic the macroscopic and microscopic architecture of the knee meniscus. *Acta Biomaterialia* **2013**, *9*, 4496–4504. [[CrossRef](#)] [[PubMed](#)]
28. Nerurkar, N.L.; Sen, S.; Huang, A.H.; Elliott, D.M.; Mauck, R.L. Engineered disc-like angle-ply structures for intervertebral disc replacement. *Spine* **2010**, *35*, 867–873. [[CrossRef](#)]
29. Li, W.-J.; Tuli, R.; Okafor, C.; Derfoul, A.; Danielson, K.G.; Hall, D.J.; Tuan, R.S. A three-dimensional nanofibrous scaffold for cartilage tissue engineering using human mesenchymal stem cells. *Biomaterials* **2005**, *26*, 599–609. [[CrossRef](#)]
30. Lebourg, M.; Sabater Serra, R.; Más Estellés, J.; Hernández Sánchez, F.; Gómez Ribelles, J.L.; Suay Antón, J. Biodegradable polycaprolactone scaffold with controlled porosity obtained by modified particle-leaching technique. *J. Mater. Sci. Mater. Med.* **2008**, *19*, 2047–2053. [[CrossRef](#)] [[PubMed](#)]
31. Li, W.-J.; Mauck, R.L.; Cooper, J.A.; Yuan, X.; Tuan, R.S. Engineering controllable anisotropy in electrospun biodegradable nanofibrous scaffolds for musculoskeletal tissue engineering. *J. Biomech.* **2007**, *40*, 1686–1693. [[CrossRef](#)] [[PubMed](#)]
32. Koepsell, L.; Remund, T.; Bao, J.; Neufeld, D.; Fong, H.; Deng, Y. Tissue engineering of annulus fibrosus using electrospun fibrous scaffolds with aligned polycaprolactone fibers. *J. Biomed. Mater. Res. Part A* **2011**, *99A*, 564–575. [[CrossRef](#)] [[PubMed](#)]
33. Koepsell, L.; Zhang, L.; Neufeld, D.; Fong, H.; Deng, Y. Electrospun nanofibrous polycaprolactone scaffolds for tissue engineering of annulus fibrosus. *Macromol. Biosci.* **2011**, *11*, 391–399. [[CrossRef](#)]
34. Thorvaldsson, A.; Stenhamre, H.; Gatenholm, P.; Walkenström, P. Electrospinning of highly porous scaffolds for cartilage regeneration. *Biomacromolecules* **2008**, *9*, 1044–1049. [[CrossRef](#)] [[PubMed](#)]
35. Hench, L.L. The story of bioglass. *J. Mater. Sci.* **2006**, *17*, 967–978. [[CrossRef](#)] [[PubMed](#)]
36. Jones, J.R. Review of bioactive glass: From hench to hybrids. *Acta Biomaterialia* **2013**, *9*, 4457–4486. [[CrossRef](#)] [[PubMed](#)]
37. Baino, F.; Hamzehlou, S.; Kargozar, S. Bioactive glasses: Where are we and where are we going? *J. Funct. Biomater.* **2018**, *9*, 25. [[CrossRef](#)] [[PubMed](#)]
38. Wilson, J.; Pigott, G.H.; Schoen, F.J.; Hench, L.L. Toxicology and biocompatibility of bioglasses. *J. Biomed. Mater. Res.* **1981**, *15*, 805–817. [[CrossRef](#)]
39. Sola, A.; Bellucci, D.; Cannillo, V. Functionally graded materials for orthopedic applications—An update on design and manufacturing. *Biotechnol. Adv.* **2016**, *34*, 504–531. [[CrossRef](#)] [[PubMed](#)]
40. Day, R.M.; Boccaccini, A.R.; Shurey, S.; Roether, J.A.; Forbes, A.; Hench, L.L.; Gabe, S.M. Assessment of polyglycolic acid mesh and bioactive glass for soft-tissue engineering scaffolds. *Biomaterials* **2004**, *25*, 5857–5866. [[CrossRef](#)] [[PubMed](#)]
41. Verrier, S.; Blaker, J.J.; Maquet, V.; Hench, L.L.; Boccaccini, A.R. PDLLA/Bioglass@composites for soft-tissue and hard-tissue engineering: An in vitro cell biology assessment. *Biomaterials* **2004**, *25*, 3013–3021. [[CrossRef](#)]
42. Stamboulis, A.; Hench, L.L.; Boccaccini, A.R. Mechanical properties of biodegradable polymer sutures coated with bioactive glass. *J. Mater. Sci. Mater. Med.* **2002**, *13*, 843–848. [[CrossRef](#)]
43. Li, H.; Chen, S.; Wu, Y.; Jiang, J.; Ge, Y.; Gao, K.; Zhang, P.; Wu, L. Enhancement of the osseointegration of a polyethylene terephthalate artificial ligament graft in a bone tunnel using 58s bioglass. *Int. Orthop.* **2012**, *36*, 191–197. [[CrossRef](#)]
44. Suominen, E.; Aho, A.J.; Vedel, E.; Kangasniemi, I.; Uusipaikka, E.; Yli-Urpo, A. Subchondral bone and cartilage repair with bioactive glasses, hydroxyapatite, and hydroxyapatite-glass composite. *J. Biomed. Mater. Res.* **1996**, *32*, 543–551. [[CrossRef](#)]
45. Bal, B.S.; Rahaman, M.N.; Jayabalan, P.; Kuroki, K.; Cockrell, M.K.; Yao, J.Q.; Cook, J.L. In vivo outcomes of tissue-engineered osteochondral grafts. *J. Biomed. Mater. Res. Part B Appl. Biomater.* **2010**, *93B*, 164–174.
46. Tellisi, N.; Ashammakhi, N. Comparison of meshes, gels and ceramic for cartilage tissue engineering in vitro. *Eur. J. Plast. Surg.* **2012**, *35*, 159–170. [[CrossRef](#)]

47. Wu, J.; Xue, K.; Li, H.; Sun, J.; Liu, K. Improvement of PHBV scaffolds with bioglass for cartilage tissue engineering. *PLoS ONE* **2013**, *8*, e71563. [[CrossRef](#)]
48. Isa, I.L.M.; Günay, B.; Joyce, K.; Pandit, A. Tissue engineering: Biomaterials for disc repair. *Curr. Mol. Biol. Rep.* **2018**, *4*, 161–172. [[CrossRef](#)]
49. Zur, G.; Linder-Ganz, E.; Elsner, J.; Shani, J.; Brenner, O.; Agar, G.; Hershman, E.; Arnoczky, S.; Guilak, F.; Shterling, A. Chondroprotective effects of a polycarbonate-urethane meniscal implant: Histopathological results in a sheep model. *Knee Surg. Sports Traumatol. Arthrosc.* **2011**, *19*, 255–263. [[CrossRef](#)]
50. Messner, K. Meniscal substitution with a teflon-periosteal composite graft: A rabbit experiment. *Biomaterials* **1994**, *15*, 223–230. [[CrossRef](#)]
51. Messner, K. The concept of a permanent synthetic meniscus prosthesis: A critical discussion after 5 years of experimental investigation using dacron and teflon implants. *Biomaterials* **1994**, *15*, 243–250. [[CrossRef](#)]
52. Anindyajati, A.; Boughton, P.; Ruys, A. Fabrication and microstructure evaluation of fibrous composite for acetabular labrum implant. *Mater. Sci. Forum* **2017**, *900*, 17–22. [[CrossRef](#)]
53. Ferro, F.P.; Philippon, M.J.; Rasmussen, M.T.; Smith, S.D.; LaPrade, R.F.; Wijdicks, C.A. Tensile properties of the human acetabular labrum and hip labral reconstruction grafts. *Am. J. Sports Med.* **2015**, *43*, 1222–1227. [[CrossRef](#)]
54. Hunter, A.; Archer, C.W.; Walker, P.S.; Blunn, G.W. Attachment and proliferation of osteoblasts and fibroblasts on biomaterials for orthopaedic use. *Biomaterials* **1995**, *16*, 287–295. [[CrossRef](#)]
55. Silver, I.A.; Erecinska, M. Interactions of osteoblastic and other cells with bioactive glasses and silica in vitro and in vivo. *Materialwissenschaft Werkstofftechnik* **2003**, *34*, 1069–1075. [[CrossRef](#)]
56. Bellucci, D.; Sola, A.; Anesi, A.; Salvatori, R.; Chiarini, L.; Cannillo, V. Bioactive glass/hydroxyapatite composites: Mechanical properties and biological evaluation. *Mater. Sci. Eng. C* **2015**, *51*, 196–205. [[CrossRef](#)]
57. Carvalho, S.; Oliveira, A.; Andrade, V.; De Fatima Leite, M.; Goes, A.; Pereira, M. Comparative effect of the ionic products from bioactive glass dissolution on the behavior of cementoblasts, osteoblasts, and fibroblasts. *Key Eng. Mater.* **2009**, 396–398, 55–59. [[CrossRef](#)]
58. Detsch, R.; Stoor, P.; Grünewald, A.; Roether, J.A.; Lindfors, N.C.; Boccaccini, A.R. Increase in VEGF secretion from human fibroblast cells by bioactive glass S53P4 to stimulate angiogenesis in bone. *J. Biomed. Mater. Res. Part A* **2014**, *102*, 4055–4061. [[CrossRef](#)] [[PubMed](#)]
59. Helen, W.; Gough, J.E. Cell viability, proliferation and extracellular matrix production of human annulus fibrosus cells cultured within pdlla/bioglass@composite foam scaffolds in vitro. *Acta Biomaterialia* **2008**, *4*, 230–243. [[CrossRef](#)] [[PubMed](#)]
60. Shih, C.-J.; Lu, P.-S.; Hsieh, C.-H.; Chen, W.-C.; Chen, J.-C. Effects of bioglass powders with and without mesoporous structures on fibroblast and osteoblast responses. *Appl. Surf. Sci.* **2014**, *314*, 967–972. [[CrossRef](#)]
61. Alcaide, M.; Portolés, P.; López-Noriega, A.; Arcos, D.; Vallet-Regí, M.; Portolés, M.T. Interaction of an ordered mesoporous bioactive glass with osteoblasts, fibroblasts and lymphocytes, demonstrating its biocompatibility as a potential bone graft material. *Acta Biomaterialia* **2010**, *6*, 892–899. [[CrossRef](#)]
62. Staniewicz-Brudnik, B.; Lekka, M.; Bączek, E.; Wodnicka, K.; Miller, T.; Wilk, W. Biocomposites with submicrocrystalline sintered corundum and bioglass system as substrates and their structural and physical properties. Short- and long-term cultures of the fibroblast human skin on these substrates. *Optica Applicata* **2012**, *42*, 387–397.
63. Day, R.M. Bioactive glass stimulates the secretion of angiogenic growth factors and angiogenesis in vitro. *Tissue Eng.* **2005**, *11*, 768–777. [[CrossRef](#)]
64. Yu, H.F.; Peng, J.L.; Xu, Y.H.; Chang, J.; Li, H.Y. Bioglass activated skin tissue engineering constructs for wound healing. *ACS Appl. Mater. Interfaces* **2016**, *8*, 703–715. [[CrossRef](#)] [[PubMed](#)]
65. Choe, J.H.; Lee, S.J.; Lee, Y.M.; Rhee, J.M.; Lee, H.B.; Khang, G. Proliferation rate of fibroblast cells on polyethylene surfaces with wettability gradient. *J. Appl. Polym. Sci.* **2004**, *92*, 599–606. [[CrossRef](#)]
66. Soon Hee, K.; Hyun Jung, H.; Youn Kyung, K.; Sun Jung, Y.; Rhee, J.M.; Moon Suk, K.; Hai Bang, L.; Khang, G. Correlation of proliferation, morphology and biological responses of fibroblasts on ldpe with different surface wettability. *J. Biomater. Sci. Polym. Ed.* **2007**, *18*, 609–622.
67. Novotná, Z.; Rimpelová, S.; Juřík, P.; Veselý, M.; Kolská, Z.; Hubáček, T.; Ruml, T.; Švorčík, V. The interplay of plasma treatment and gold coating and ultra-high molecular weight polyethylene: On the cytocompatibility. *Mater. Sci. Eng. C* **2017**, *71*, 125–131. [[CrossRef](#)] [[PubMed](#)]

68. Rimpelová, S.; Kasálková, N.S.; Slepíčka, P.; Lemerová, H.; Švorčík, V.; Ruml, T. Plasma treated polyethylene grafted with adhesive molecules for enhanced adhesion and growth of fibroblasts. *Mater. Sci. Eng. C* **2013**, *33*, 1116–1124. [[CrossRef](#)] [[PubMed](#)]
69. Soparkar, C.N.S.; Wong, J.F.; Patrinely, J.R.; Appling, D. Epidermal and fibroblast growth factors enhance fibrovascular integration of porous polyethylene implants. *Ophthalmic Plast. Reconstr. Surg.* **2000**, *16*, 337–340. [[CrossRef](#)]
70. Anindyajati, A.; Boughton, P.; Ruys, A. The effect of rotating collector design on tensile properties and morphology of electrospun polycaprolactone fibres. *MATEC Web Conf.* **2015**, *27*, 02002. [[CrossRef](#)]
71. Roether, J.A.; Boccaccini, A.R.; Hench, L.L.; Maquet, V.; Gautier, S.; Jerjme, R. Development and in vitro characterisation of novel bioresorbable and bioactive composite materials based on polylactide foams and bioglass for tissue engineering applications. *Biomaterials* **2002**, *23*, 3871–3878. [[CrossRef](#)]
72. Stamboulis, A.G.; Boccaccini, A.R.; Hench, L.L. Novel biodegradable polymer/bioactive glass composites for tissue engineering applications. *Adv. Eng. Mater.* **2002**, *4*, 105–109. [[CrossRef](#)]
73. Chatterjee, K.; Hung, S.; Kumar, G.; Simon, C.G. Time-dependent effects of pre-aging 3D polymer scaffolds in cell culture medium on cell proliferation. *J. Funct. Biomater.* **2012**, *3*, 372–381. [[CrossRef](#)]
74. Thevenot, P.; Nair, A.; Dey, J.; Yang, J.; Tang, L. Method to analyze three-dimensional cell distribution and infiltration in degradable scaffolds. *Tissue Eng. Part C Methods* **2008**, *14*, 319–331. [[CrossRef](#)]
75. Sobieraj, M.C.; Rinnac, C.M. Ultra high molecular weight polyethylene: Mechanics, morphology, and clinical behavior. *J. Mech. Behav. Biomed. Mater.* **2009**, *2*, 433–443. [[CrossRef](#)] [[PubMed](#)]
76. Theodorou, G.; Goudouri, O.M.; Kontonasaki, E.; Chatzistavrou, X.; Papadopoulou, L.; Kantiranis, N.; Paraskevopoulos, K.M. Comparative bioactivity study of 45S5 and 58S bioglasses in organic and inorganic environment. *Bioceram. Dev. Appl.* **2011**, *1*, 4. [[CrossRef](#)]
77. Chen, Q.Z.; Efthymiou, A.; Salih, V.; Boccaccini, A.R. Bioglass®-derived glass–ceramic scaffolds: Study of cell proliferation and scaffold degradation in vitro. *J. Biomed. Mater. Res. Part A* **2008**, *84A*, 1049–1060. [[CrossRef](#)] [[PubMed](#)]
78. Rohanova, D.; Boccaccini, A.R.; Horkavcova, D.; Bozdechova, P.; Bezdicka, P.; Castoralova, M. Is non-buffered DMEM solution a suitable medium for in vitro bioactivity tests? *J. Mater. Chem. B* **2014**, *2*, 5068–5076. [[CrossRef](#)]
79. Gorustovich, A.A.; Roether, J.A.; Boccaccini, A.R. Effect of bioactive glasses on angiogenesis: A review of in vitro and in vivo evidences. *Tissue Eng. Part B Rev.* **2010**, *16*, 199–207. [[CrossRef](#)] [[PubMed](#)]
80. Silva, M.; Shepherd, E.F.; Jackson, W.O.; Dorey, F.J.; Schmalzried, T.P. Average patient walking activity approaches 2 million cycles per year. *J. Arthroplast.* **2002**, *17*, 693–697. [[CrossRef](#)]
81. Reznickova, A.; Novotna, Z.; Kolska, Z.; Kasalkova, N.S.; Rimpelova, S.; Svorcik, V. Enhanced adherence of mouse fibroblast and vascular cells to plasma modified polyethylene. *Mater. Sci. Eng. C* **2015**, *52*, 259–266. [[CrossRef](#)]
82. Matsuda, T.; Yamauchi, K.; Ito, G. The influence of bioglass on the growth of fibroblasts. *J. Biomed. Mater. Res.* **1987**, *21*, 499–507. [[CrossRef](#)]

